# MODELLING OF TROPICAL CYCLONES AND APPLICATIONS TO MEDITERRANEAN SEA

A THESIS SUBMITTED TO
THE GRADUATE SCHOOL OF NATURAL AND APPLIED SCIENCES
OF
MIDDLE EAST TECHNICAL UNIVERSITY

BY

ASLIHAN DEVRAN

IN PARTIAL FULFILLMENT OF THE REQUIREMENTS
FOR
THE DEGREE OF MASTER OF SCIENCE
IN
CIVIL ENGINEERING

NOVEMBER 2022

Approval of the thesis:

**MODELLING OF TROPICAL CYCLONES AND APPLICATIONS TO MEDITERRANEAN SEA**

submitted by **ASLIHAN DEVRAN** in partial fulfillment of the requirements for the degree of **Master of Science** i**n Civil Engineering, Middle East Technical University** by,

Prof. Dr. Halil Kalıpçılar
Dean, Graduate School of **Natural and Applied Sciences** _____

Prof. Dr. Erdem Canbay
Head of the Department, **Civil Engineering** _____

Prof. Dr. Ahmet Cevdet Yalçıner
Supervisor, **Civil Engineering, METU** _____

**Examining Committee Members:**

Assist. Prof. Dr. Cüneyt Baykal
Civil Engineering, METU _____

Prof. Dr. Ahmet Cevdet Yalçıner
Civil Engineering, METU _____

Assist. Prof. Dr. Gülizar Özyurt Tarakcıoğlu
Civil Engineering, METU _____

Assoc. Prof. Dr. Elif Oğuz
Civil Engineering, METU _____

Assist. Prof. Dr. Alp Küçükosmanoğlu
Civil Engineering, Burdur Mehmet Akif Ersoy University _____

Date: 21.11.2022

**I hereby declare that all information in this document has been obtained and presented in accordance with academic rules and ethical conduct. I also declare that, as required by these rules and conduct, I have fully cited and referenced all material and results that are not original to this work.**

Name Last name : Aslıhan Devran

Signature :

## ABSTRACT

### MODELLING OF TROPICAL CYCLONES AND APPLICATIONS TO MEDITERRANEAN SEA

Devran, Aslıhan
Master of Science, Civil Engineering
Supervisor : Prof. Dr. Ahmet Cevdet Yalçıner

November 2022, 68 pages

Tropical cyclones occur in the tropical areas in general. Mediterranean hurricanes are cyclones with tropical characteristics and known as medicanes which occasionally develop in the Mediterranean Sea. The long waves in tropical cyclones are generated by atmospheric pressure disturbance and surface wind fields. Pressure and wind data are available in international data sources CFSR and ECMWF ERA5. This study is carried out to simulate tropical cyclones using the numerical modelling NAMI DANCE and compare the results of computed water levels with the observations and measurements. The correlation between CFSR and ECMWF ERA5 data of atmospheric pressure and wind fields is also investigated for comparison. As the case studies firstly, the numerical modelling is applied to the tropical cyclone event Dorian from 28 August to 10 September 2019 and the results are compared with the observations and measurements. Secondly, Mediterranean storms Medicane Trudy from 11 November to 14 November 2019 and Medicane Zorbas from 28 August to 30 September 2018 are simulated. The results of computed ocean waves are compared with the measurements from tide gauge stations. The results are presented with comparisons and discussions.



Keywords: Tropical cyclone, Tropical-like cyclone, Medicanes, Storm Surge, Zorbas

# ÖZ

## TROPİKAL SİKLONLARIN MODELLENMESİ VE AKDENİZ'E UYGULAMALARI

Devran, Aslıhan
Yüksek Lisans, İnşaat Mühendisliği
Tez Yöneticisi: Prof. Dr. Ahmet Cevdet Yalçıner

Kasım 2022, 68 sayfa

Tropikal siklonlar genel olarak tropikal bölgelerde meydana gelir. Akdeniz kasırgaları, Akdenizde zaman zaman gelişen, tropikal özelliklere sahip siklonlardır. Akdeniz kıyıları, daha sık ve güçlü siklonlar nedeniyle her geçen gün daha savunmasız hale gelmektedir. Tropikal siklonlar uzun dalgalar, atmosferik basınç değişikliği ve yüzey rüzgar alanları tarafından üretilir. Basınç ve rüzgar verileri, uluslararası veri kaynakları CFSR ve ECMWF ERA5 içinde mevcuttur. Bu çalışma, NAMI DANCE sayısal modellemesini kullanarak tropikal siklonları simüle etmek ve hesaplanan dalgaların sonuçlarını gözlem ve ölçümlerle karşılaştırmak için yapılmıştır. Atmosferik basınç ve rüzgar alanlarının CFSR ve ECMWF ERA5 verileri arasındaki korelasyonu da karşılaştırma için incelenmiştir. Örnek olay çalışmalarından ilk olarak, Dorian 28 Ağustos 10 Eylül 2019 tropikal siklon olayına sayısal modelleme uygulanmış ve sonuçlar gözlem ve ölçümlerle karşılaştırılmıştır. İkinci olarak, Trudy 11 Kasım 14 Kasım 2019 ve Zorbas 28 Ağustos 30 Eylül 2018 Akdeniz fırtınaları simüle edilmiştir. Hesaplanan okyanus dalgalarının sonuçları, gelgit ölçüm istasyonlarından alınan ölçümlerle karşılaştırarak sunulmuştur.

Anahtar Kelimeler: Tropikal Siklon, Tropikal-benzeri Siklon, Akdeniz Kasırgası, Fırtına Kabarması, Zorba

To my grandmother, in loving memory

## ACKNOWLEDGMENTS

Firstly, I would like to express my sincere gratitude to my supervisor, Prof. Dr. Ahmet Cevdet Yalçıner, for all of his help, kindness and supervision throughout the course of my master's degree and the research.

I am would like to thank Prof. Dr. Ayşen Ergin for her guidance starting from my undergraduate years.

I would like to to thank Assist. Prof. Dr. Cüneyt Baykal for his help and guidance of my studies in coastal and ocean engineering.

I would like to thank Assist. Prof. Dr. Gülizar Özyurt Tarakcıoğlu her help and guidance of my studies in coastal and ocean engineering.

I am gratefully thankful to Dr. Işıkhan Güler for his support and kindness throughout my master's degree.

I would like to thank Dr. Gözde Güney Doğan Bingöl for her patience, kindness, support and supervision to my research.

I would like to thank Dr. Gökhan Güler for his help and guidance starting from my undergraduate years.

I would like to thank Prof. Dr. Giovanni Scicchitano for helping me to access the digital numeric data.

I would like to thank Gökçe Ömeroğlu for her contribution to my research.

Special thanks to Bora Yalçıner for his valuable contributions to my research.

Also, many thanks go on to my Coastal Engineering family.

Finally, my lovely family and boyfriend deserve the sincerest gratitude for their love, tolerance, and support during every stage of my life.

## TABLE OF CONTENTS

## LIST OF TABLES

TABLES

## LIST OF FIGURES

FIGURES

# CHAPTER 1

## INTRODUCTION

Any disrupted condition in an environment or an astronomical body's atmosphere, particularly one that affects its surface and strongly suggests severe weather, is referred to as a storm, and it can be in the form of cyclones, thunderstorms, tornadoes, and rainstorms. Tropical cyclones are the one of the greatest risks to life and property. They are composed of a variety of hazards, including storm surges, floods, and powerful winds. Together, these risks combine and significantly raise the possibility of fatalities and property damage. Tropical cyclones have been accused of 1942 catastrophes over the previous fifty years, which resulted in 779 324 fatalities and US$ 1407.6 billion in economic losses (World Meteorological Organization, 2021).

A tropical cyclone can be defined as a rotating storm that forms from tropical oceans and receives energy there. Its diameter is from 200 to 500 km on average, but it can be up to 1000 km. In the Northern Hemisphere, the wind blows counterclockwise, whereas, in the Southern Hemisphere, it blows clockwise.

Depending on where it occurs, this weather phenomenon has many names. For example, “hurricane” is called when it occurs in the Atlantic Ocean and the eastern and central North Pacific Ocean; “tropical cyclone” is called when it occurs in the southwest Indian Ocean.

Tropical cyclone reaction to a changing climate has attracted much attention and research (Moon, J. et al., 2018). The Mediterranean region is one of the regions identified as being most vulnerable to climate change (Giorgi, F., 2006). Therefore, it is believed that variations in cyclone occurrence and features will be significant in historical, current, and future changes to the Mediterranean climate. (Nissen,

K.M. et al. 2012). Many studies investigate tropical cyclones' behavior under the influence of climate change. It is becoming more evident that tropical storm means and maximum intensities could be affected by climate change (Walsh, K. et al., 1999). Consequently, more intense cyclone events are observed in the Mediterranean Sea.

In this study, the selected tropical cyclones and storm events in the Mediterranean Sea are modelled and results are compared with different data sets and also actual measurements from gauge points. The numerical model is built up on the tsunami numerical model NAMI DANCE and its inputs include bathymetry, pressure field (spatial and temporal) and wind field. Data required for the model is taken from CFSR and ECMWF.

The main objectives of this study: compare the two data sets of different resources with each other, discuss the agreement of the pressure and wind speed of two data sources, simulate tropical cyclones and compute consecutive ocean waves and compare computed water level data with observations or measurements.

As the case studies firstly, the numerical modelling is applied to the tropical cyclone Dorian (24 August-10 September 2019) and the results are compared with the observations and measurements. It is noticeable that models often follow a similar pattern. After that, CFSR and ECMWF data sources were used for Mediterranean Sea applications which are Medicane Zorbas (September 2018) and Medicane Trudy (November 2019). The results were presented and interpreted in discussions.

Chapter 2 provides information about current studies on tropical cyclone numerical modelling applications.

Chapter 3 provides information about forecast data sources, CFSR, ECMWF and HRES, their prevalence, features and resolution.

In Chapter 4, tropical cyclone Dorian was summarized particularly with the help of National Hurricane Center Tropical Cyclone Report.

Chapter 5 introduces numerical modeling of NAMIDANCE and provides a brief explanation of the model's theoretical background.

Chapter 6 gives information about the numerical model application to tropical cyclone Dorian with specific gauge points, bathymetry source, grid size for each domain. It also contains pressure and wind fields for the stations and their comparison with two different data sources. Furthermore, for the verification of the model as an output data computed water levels for all three data sets (ECMWF, CFSR, HRES) and measured values at every gauge point are compared.

Chapter 7 gives information about the numerical model applied to the Mediterranean Sea. Medicane Trudy (November 2019) and Medicane Zorbas (September 2018) are modeled and their gauge points, bathymetry source and grid size for each domain. It also contains pressure and wind fields for stations and their comparison with two different data sources and actual measurements. Besides, as output data, water level elevation with two data sets (ECMWF, CFSR) and measured values at every gauge point are compared.

# CHAPTER 2

# LITERATURE REVIEW

Mediterranean hurricanes are the cyclones with tropical characteristics and known as medicanes which occasionally develop in the Mediterranean Sea. The Mediterranean coasts are becoming more vulnerable to coastal erosion, particularly as a result of the more frequent and powerful Medicanes. They have a significant potential for damage like storm surges and tsunamis, consequently accurate simulations of their evolution in climate scenarios are essential for a sufficient response to climate change. Numerous studies employing various methods have been made on numerical modeling of tropical cyclones, storm surges and tsunamis An overview of the most current studies are summarized in the following.

Fernández and Alemán et. al. (2020) used numerical modeling ROM to investigate the ocean-atmosphere coupled models that reflect the medicanes more accurately, particularly in frequency and intensity. ROM, regionally-coupled model indicates air-sea interactions affect the evolution of tropical cyclones in future climate projections. The climate simulations under the selected scenario have a total frequency decline that is greater in magnitude in the linked configuration than in the uncoupled one, although the density shows varied varying behavior according to coupling. The proportional frequency of higher-intensity tropical cyclones rises in the coupled simulation however, it is not the case in the uncoupled run. Additionally, results shows that the linked model replicates the summertime low for tropical cyclone occurrence more accurately than the uncoupled model, which avoids recreating the summer's unreasonably severe events.

Using a storm surge-wave-tide coupled model, Siahsarani et al. (2021) carried out numerical simulations of tropical cyclone-induced storm surge in the Gulf of

Oman. A storm surge is a complicated process that involves the interaction of current, tide, and waves. Although the wind is the main cause of the surge, waves and tide also significantly contribute to its momentum and mass movement. Despite its sensitivity to storms and coastal threats, the interaction of waves with storm surge has not yet been studied in the Iranian Makran coastal region of the Gulf of Oman. This study aims to analyze tropical cyclone-induced waves and storm surges in the Gulf of Oman using the wave-tide-circulation coupled system. The two-way coupling of wave and hydrodynamic models as MIKE 21 SW and MIKE 3 HD were used to run simulations to determine the wave characteristics and water levels during the super storm Gonu. These simulations were confirmed using field observations. The water level and significant wave height predicted by the model, in particular, were in good agreement with what was observed during the Gonu storm. The key findings of this study emphasize the importance of wave-induced setup caused by radiation stress as well as the part played by the coupled model's inaccurate storm surge simulation.

Scicchitano and Tarascio et al. (2020) recreated pre and post-immersive virtual scenarios in order to geometrically analyze the video and ascertain flow velocity and wave heights at the time of boulder displacements using various survey and remote sensing techniques during the impact of Medicane Zorbas on Southeast Sicily. The assessment of these models has been complicated by the absence of real movement observations during the past several years despite the fact that numerous writers have published competing hypotheses to explain how boulders respond to large waves. The recent rise of internet video-sharing platforms in coastal areas has made it feasible to observe the development of rocky beaches during storm occurrences. A surveillance camera in the Marine Protected Area of Plemmirio recorded the movement of many stones along the shore of the Maddalena Peninsula in Siracusa, Southeast Sicily, during the landing of the Medicane Zorbas in September 2018. Uncrewed autonomous vehicle photogrammetric and terrestrial laser scanner surveys were conducted to recreate realistic virtual environments and

geometrically evaluate the boulder displacements seen on camera. Studies revealed that the displacements weren't brought on by a single enormous wave, but rather by the clash of multiple smaller waves that buried the boulders. The figures of flow density and lift coefficient cited in the literature are overestimated, as shown by a comparison of the flow velocities predicted using relationships with those acquired from movies.

The September 2018 impacts of Medicane Zorbas were recreated by Scicchitano and Scardino et al. (2021) using post-event geomorphological surveys, direct witness interviews, and analysis of surveillance system or social media footage. Between the Thapsos Peninsula and Marzamemi, seven coastal sites were able to be assessed for the level of flooding. Although the flooding from Zorbas looks to be greater than that from the region's major seasonal storms between the years of 2015-2019, it is comparable to that from Medicane Qendresa, which struck Sicily. Tropical cyclones in Mediterranean region produce more potential risk for flooding than yearly storms because they can cause a higher and longer surge along the coastline, according to wave propagation and extreme water level modeling completed for the main storm events that occurred in the region since 2005 and analyses of data recorded by tide gauges in Catania, Porto Palo di Capo Passero. The findings underlined the need to more thoroughly assess the coastal hazard associated with Medicanes' spread, particularly in light of the effects of climate change, which will likely cause these occurrences to be more intense and last longer compared to how they currently.

Fritz and Blount et. al. (2010) simulated storm surge of Gonu one of the strongest tropical cyclone in the Arabian Sea by using Advanced Circulation Model (ADCIRC). Due to wadi floods, storm surge, and storm wave impact, Gonu caused coastal damage. From August 1 to August 4, 2007, high water marks, overland flow depths, and inundation distances were observed in the coastal flood zones around the Gulf of Oman. The eastern tip of Oman, Ras al-Hadd, saw the highest

highwater marks, which exceeded 5 meters. By contrasting the Cyclone Gonu observations with those from the Indian Ocean Tsunami of 2004, the multi-hazard component is examined. The modeling results demonstrate a peak storm surge distribution trend with decreasing storm surge from Ras al-Hadd to Muscat that is similar to the observed high water mark distribution. Model output predicts a storm surge of more than 1 m between Ras al-Hadd and Quriat, peaking at 1.51 m. Wave motion and overland flow may be primarily to blame for the disparity between high water marks and model results. The storm surge model still has to be connected with a short-wave model, which will increase the predicted storm surge.

Miglietta (2019) mentioned in his article that studying the sensitivity of the simulations to various factors and forcings is crucial since the correct prediction of Medicanes is a significant issue for numerical weather prediction models. Numerous research is necessary to describe cyclones in numerical models better and evaluate how they evolve in various environmental situations. For instance, in numerical simulations using the WRF (Weather Research and Forecasting) Model the initial conditions were the primary determinants of the cyclone depth and trajectory. Moreover, previous studies with the WRF model and COAWST (Coupled Ocean-Atmosphere-Waves-Sediment Transport) modelling system support earlier research that coupled models are better capable than atmospheric standalone numerical systems for comprehensive and in-depth investigations of Medicanes and can be helpful tools for climate forecasts.

# CHAPTER 3

## DATA SOURCES FOR TROPICAL CYCLONES

The Climate Forecast System Reanalysis called as CFSR is a product of the third generation of reanalysis. It is a global, high-resolution coupled atmosphere-ocean-land surface-sea ice system that aims to provide the most accurate approximation of the status of these coupled domains over time. The hourly data set CFSR Version 2 is used to simulate how oceans, atmosphere, and land interact. (National Centers for Environmental Prediction, 2011).

The European Centre for Medium-Range Weather Forecasts called as ECMWF is an international organization with 35 member countries. The European Centre for Medium-Range Weather Forecasting (ECMWF) is a research institute as well as a twenty-four hour operating service that produces and distributes numerical weather forecasts to its Member States. The national meteorological services in the Member States have complete access to this data. The Centre also sells a catalog of forecast data to enterprises and other commercial customers all over the world. ERA5 is open-source data that provides hourly estimates for a wide range of atmospheric, terrestrial, and oceanic climate variables. The data cover the Earth on a 30km grid and resolve the atmosphere with 137 levels ranging from the surface to 80km in altitude. At decreased geographical and temporal resolutions, ERA5 offers information concerning uncertainty for all variables. The High-Resolution Forecast (HRES) data from the European Centre for Medium-Range Weather Forecasts (ECMWF) were utilized as meteorological data, specifically, hourly mean sea level pressure and wind data above ten meter high of sea level. HRES data is only available for the Dorian event.

Figure 3.1 shows that the minimum sea level pressure was 999 mb in HRES data on September 2, 2019 at 00:00 UTC. Also, maximum eastward wind (u10) was

between the range of -46 m/s and 36 m/s (u10); northward wind data (v10) was between -37 m/s and 42 m/s.

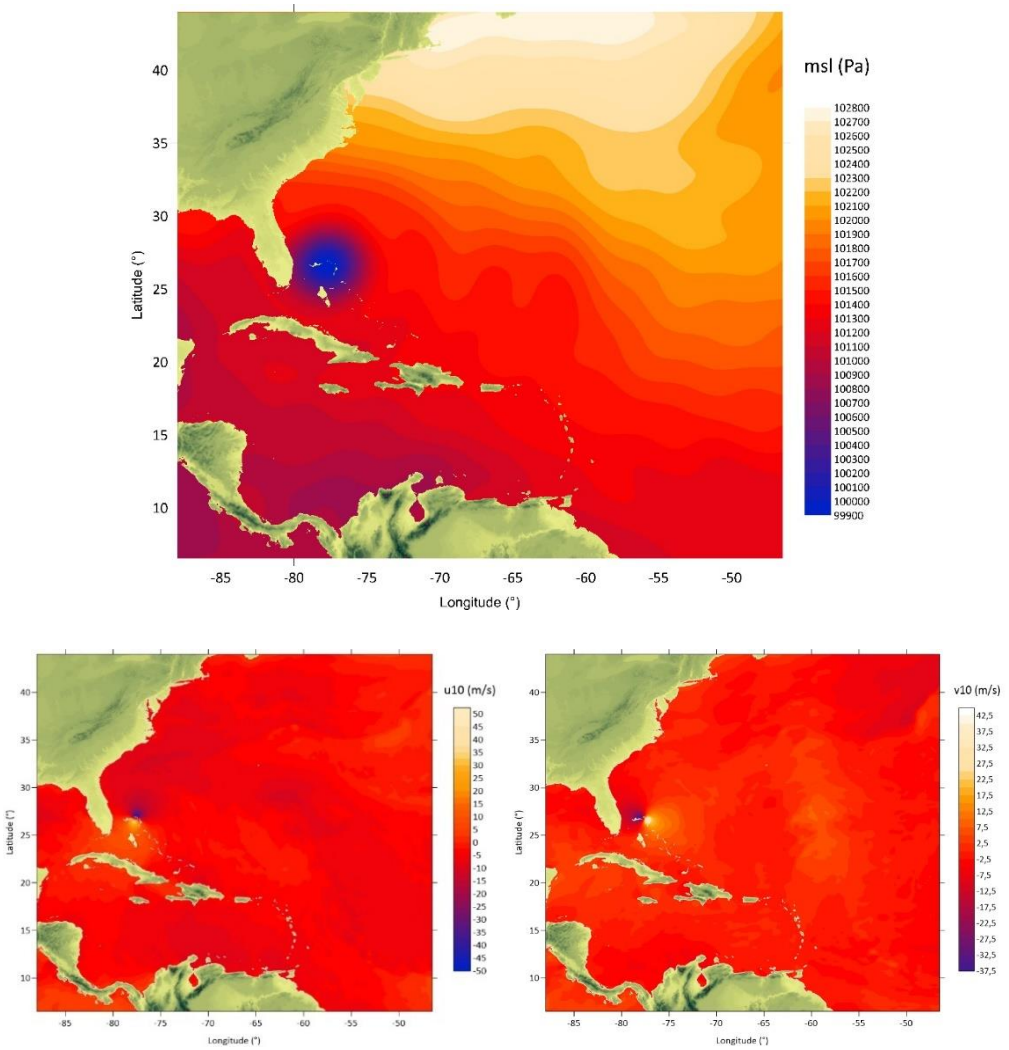


Figure 3.1. The atmospheric pressure (msl), eastward wind (u10) and northward wind data (v10) of HRES data set on September 2, 2019 at 00:00 UTC

# CHAPTER 4

## TROPICAL CYCLONE DORIAN

The tropical cyclone that emerged on Africa's west coast on August 19, 2019 proceeded westward over the tropical Atlantic, although storm activity decreased in the meanwhile. On August 22, the satellite-observed cyclonic circulation revealed that a convection field had formed near 40° West. This energy became a tropical depression, then a tropical storm, on August 24th. Hurricane Dorian's route is seen in Figure 4.1.

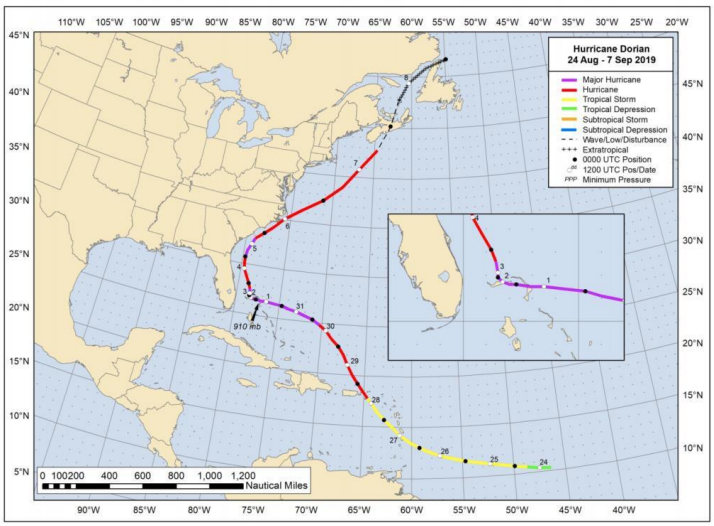


Figure 4.1. Track of Hurricane Dorian (NOAA, National Hurricane Center, 2020).

At 16:40 UTC on 1 September, Dorian had become a category five hurricane with predicted winds of 1296 km and a minimum pressure of 91000 Pa shown in Figure 4.2 and Figure 4.3.

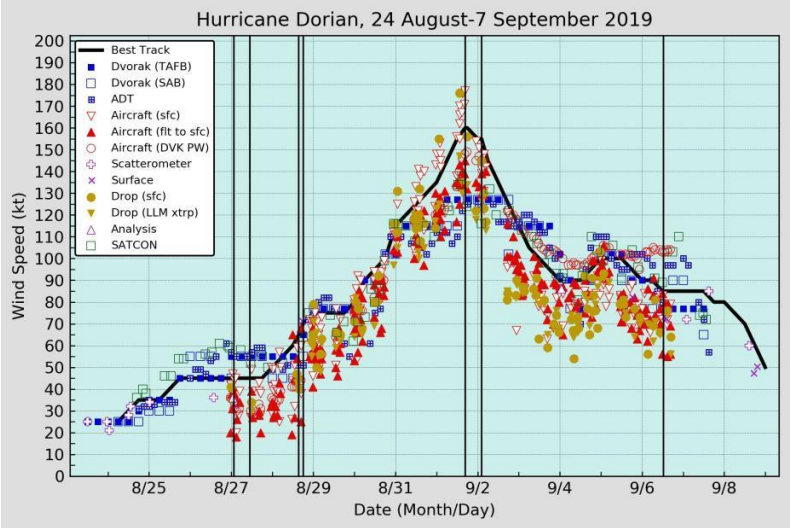


Figure 4.2. The observations of wind speed with the best track (NOAA, National Hurricane Center, 2020)

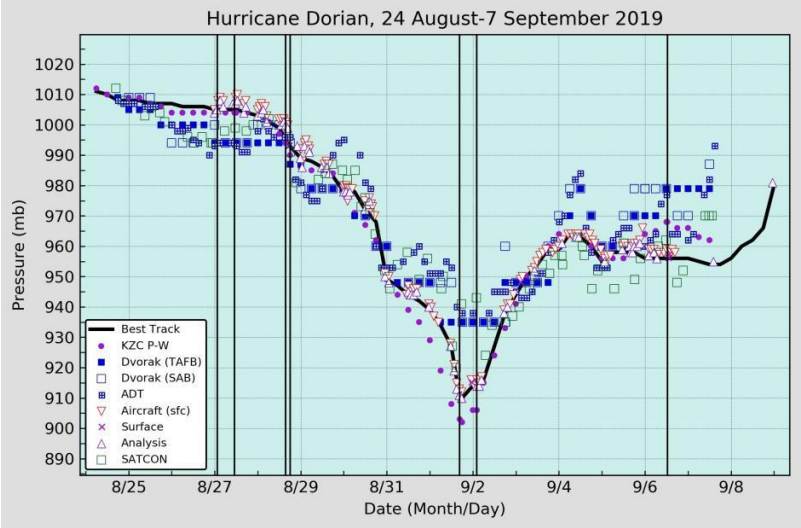


Figure 4.3. The observations of central pressure with the best track (NOAA, National Hurricane Center, 2020)

Besides the United States and Canada, the Bahamas was the region hit worst by Hurricane Dorian. According to the Bahamas' Health Minister, at than 200 persons are believed to have died in Dorian. The total was expected to be 74 by the Bahamas Weather Service (63 in Abaco and 11 in Grand Bahama). A total of 245

individuals have gone missing, according to reports. Furthermore, about 75% of the homes were severely destroyed (Figure 4.4 and Figure 4.5).

Figure 4.4. North Carolina after Hurricane Dorian (NOAA, National Hurricane Center, 2020)

Figure 4.5. North Carolina after Hurricane Dorian (NOAA, National Hurricane Center, 2020)

Inundation levels of 0.6 m to 0.9 m above ground level were recorded north of North Carolina in the Hampton Roads area of Virginia. The NOS tidal gauge at the

Chesapeake Bay entry reported a maximum water level of 1 m MHHW, while a gauge at Sewells Point in Norfolk, Virginia recorded a maximum water level of 0.95 m MHHW. Hurricane Dorian caused chaos on the US Virgin Islands, Puerto Rico, the Bahamas, Florida, Georgia, South Carolina, North Carolina, and Virginia, causing inundation and storm surge flooding throughout the coast. At the University of Hawaii Sea Level Center (UHSLC) on the Grand Bahama Islands, the measured water level was 1.95 m above Mean Higher High Water Sea level. Higher water levels occurred farther east on Grand Bahama Island but there are no tidal gauge readings available from those regions.

# CHAPTER 5

# NUMERICAL MODELLING OF TROPICAL CYCLONES

Profs. Andrey Zaytsev, Ahmet Yalciner, Anton Chernov, Efim Pelinovsky, and Andrey Kurkin created NAMI DANCE specifically for tsunami simulation. It simulates tsunami generation, propagation, coastal amplification and inundation processes. It is coded in the C++ programming language and employs the same leap-frog technique numeric solution method as TUNAMI-N2 (Imamura, 1989; Shuto, Goto, and Imamura, 1990). All tsunami parameters can be computed using NAMIDANCE. Also, it visualize the propagation of tsunami from source to destination, including inundation, and it post processing features to plot 3D graphs of sea state at chosen time intervals from various camera locations. There are three primary input data in NAMI DANCE: bathymetry, pressure field and wind field, as shown in Figure 5.1.

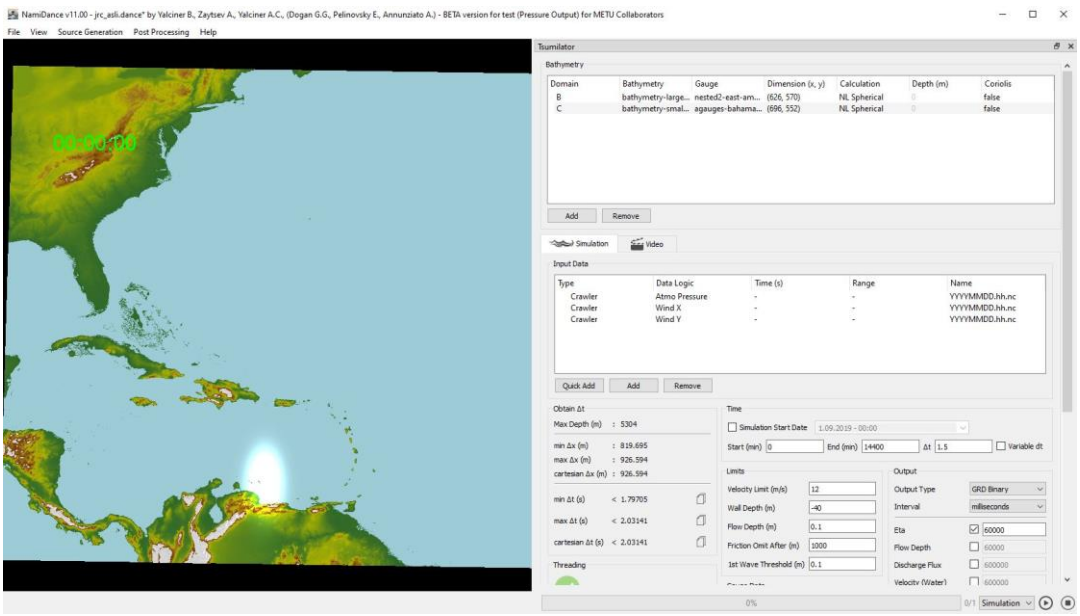


Figure 5.1. NAMI DANCE Simulation

The flow in vertical scale has no impact on the distribution of pressure in the long waves theory. The conservation of mass and momentum in a three-dimensional case is represented by the following system of equations relying on this approach and ignoring vertical acceleration.

NAMI DANCE has been upgraded to NAMI DANCE SUITE, which now includes the ability to use the graphic card's Graphical Processing Unit. It calculates (i) maximum positive amplitude, (ii) maximum flow depth, (iii) maximum current velocity, (iv) maximum momentum flux, (v) maximum hydrodynamic forces, (vi) maximum negative amplitude, (vii) maximum wave arrival time, (viii) initial wave arrival time, and (ix) durations of inundation and shoreline withdrawal which are the essential hydrodynamic parameters for long waves (Yalciner et al., 2015; Sozdinler et al., 2015; Yalciner and Zaytsev, 2017; Yalciner et al., 2017).

Equations introduce a set of two-dimensional equations in Cartesian coordinates with atmospheric pressure and wind field terms :

$$\frac{\partial \eta}{\partial t}+\frac{\partial M}{\partial x}+\frac{\partial N}{\partial y}=0$$

$$\frac{\partial M}{\partial t}+\frac{\partial}{\partial x}\left(\frac{M^2}{D}\right)+\frac{\partial}{\partial y}\left(\frac{MN}{D}\right)+gD\frac{\partial \eta}{\partial x}+\frac{\tau_x}{\rho_w}+\frac{D}{\rho_w}\frac{\partial P_{atm}}{\partial x}-\frac{\rho_{air}C_D}{\rho_w}U_{w10}\sqrt{U^2{}_{w10}+V^2{}_{w10}}=0$$

$$\frac{\partial N}{\partial t}+\frac{\partial}{\partial x}\left(\frac{MN}{D}\right)+\frac{\partial}{\partial y}\left(\frac{N^2}{D}\right)+gD\frac{\partial \eta}{\partial y}+\frac{\tau_y}{\rho_w}+\frac{D}{\rho_w}\frac{\partial P_{atm}}{\partial y}-\frac{\rho_{air}C_D}{\rho_w}V_{w10}\sqrt{U^2{}_{w10}+V^2{}_{w10}}=0$$

Table 5.1 NAMI DANCE Equations Meanings

| Symbol | Description |
|---|---|
| t | Time |
| x - y | Spatial coordinates |
| $\eta$ | Surface elevation of water |
| $\rho_w$ | Density of water |

| | |
|---|---|
| $\rho_{air}$ | Density of air |
| D | Depth of water |
| $P_{atm}$ | Atmospheric pressure |
| $\tau_x$, $\tau_y$ | Shear stresses of bottom |
| $U_{w10}, V_{w10}$ | Wind velocities in Easting and Northing directions |
| $C_D$ | Drag coefficient of wind |

$$C_D = (0.75 + 0.067(U_{w10} - u)) \cdot 10^{-3} \quad \text{for} \quad U_{w10} \le 26 \text{ m/s (Garrat, 1977)}$$

$$C_D = 2.18 \cdot 10^{-3} \quad \text{for} \quad U_{w10} > 26 \text{ m/s} \quad \text{(Powell et al. 2003)}$$

where M and N are the discharge fluxes in the x and y directions:

$$M = \int_{-h}^{\eta} u dz = u\left(D + \eta\right) = uD, \qquad N = \int_{-h}^{\eta} v dz = v\left(D + \eta\right) = vD.$$

In above equation, u and v are the water current velocities in x and y directions (horizontal plane), respectively. The bottom shear stresses are computed using following equations.

$$\frac{\tau_x}{\rho} = \frac{f_b n^2}{(\eta + D)^{7/3}} M\sqrt{M^2 + N^2}$$

$$\frac{\tau_y}{\rho} = \frac{f_b n^2}{(\eta + D)^{7/3}} N\sqrt{M^2 + N^2}$$

where fb denotes the bottom friction, which is 0.015, and Manning's coefficient n is calculated following equation.

$$n = \sqrt{\frac{f_b(\eta + D)^{1/3}}{2g}}$$

Because Coriolis force and friction are not involved in analytical solution, they are not involved in the numerical tests for accurate comparisons with analytical solution.

In the numerical model, in addition to standard inputs (bathymetry, initial water surface displacement, and fluxes if needed), the spatial distribution of the barometric pressure at the sea level in Pascal at one-minute intervals during the simulations is employed. As a set of output parameters, NAMI DANCE SUITE computes water surface elevations, magnitude and directions of water current velocities, momentum fluxes, overland flow depths throughout the domain at specified time intervals, and extremums of all these parameters. Additionally, the inundation and withdrawal limits of the shoreline motion; and time histories of these parameters at specified numerical wave gauge locations are computed.

The spatial distribution of the barometric pressure at sea level in Pascal at one-minute intervals is used in the numerical model, in comparison to basic inputs (bathymetry, initial water surface displacement, and fluxes if needed). NAMI DANCE SUITE computes water surface elevations, magnitude and directions of water current velocities, momentum fluxes, overland flow depths throughout the domain at specified time intervals, and extremums of all these parameters as a set of output parameters. Furthermore, the inundation and withdrawal limits of shoreline motion are estimated, as well as time histories of these parameters at specific numerical wave gauge locations.

# CHAPTER 6

## APPLICATION TO TROPICAL CYCLONE DORIAN

The simulation is performed using the meteorological (pressure and wind field) data from 1 September 2019 to 10 September 2019. It takes 14400 minutes in total and Δt (time interval) is chosen as 1.5 seconds. Input data includes wind and pressure data, as well as bathymetry and gauges for the B and C domains. ECMWF (ERA5) data and HRES data are both hourly and with 0.25° x 0.25° grid resolution, whereas CFSR data is hourly with 0.5° x 0.5° grid resolutions. Domain B is the coarse area and encloses National Ocean Service stations. Domain C is enclosed with "Bahamas," being which the National Hurricane Center claims to be the most severely devastated region, shown as Point 1 in Figure 6.1. The bathymetry data of Domain B and C information are shown in Table 6.1 and come from the GEBCO (General Bathymetric Chart of the Oceans) website, a free resource.

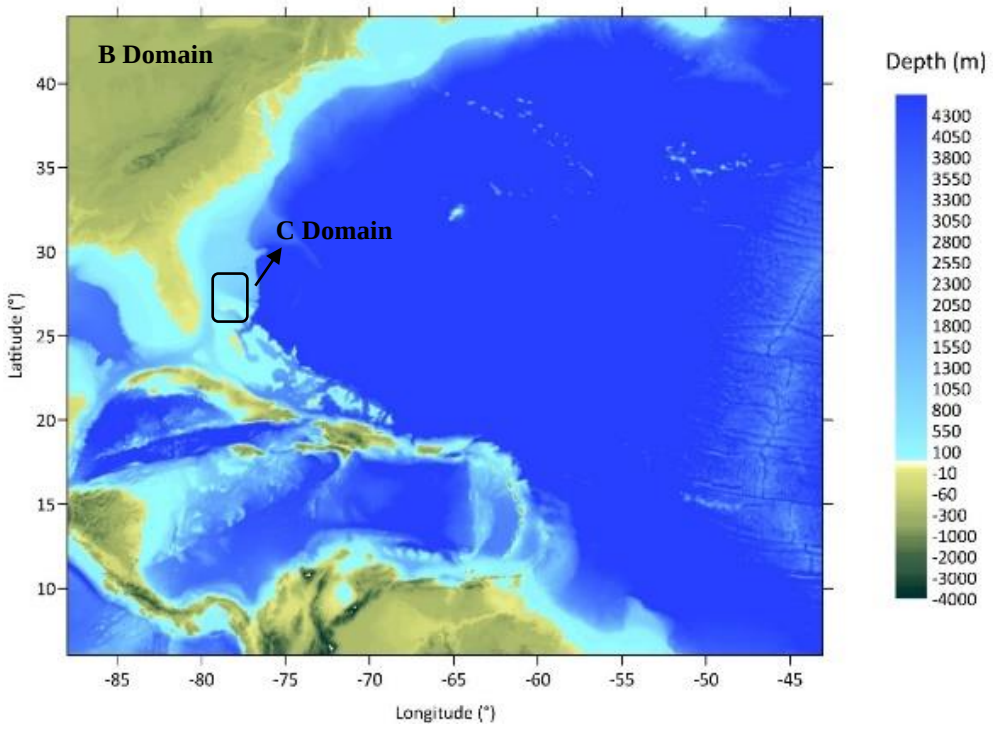

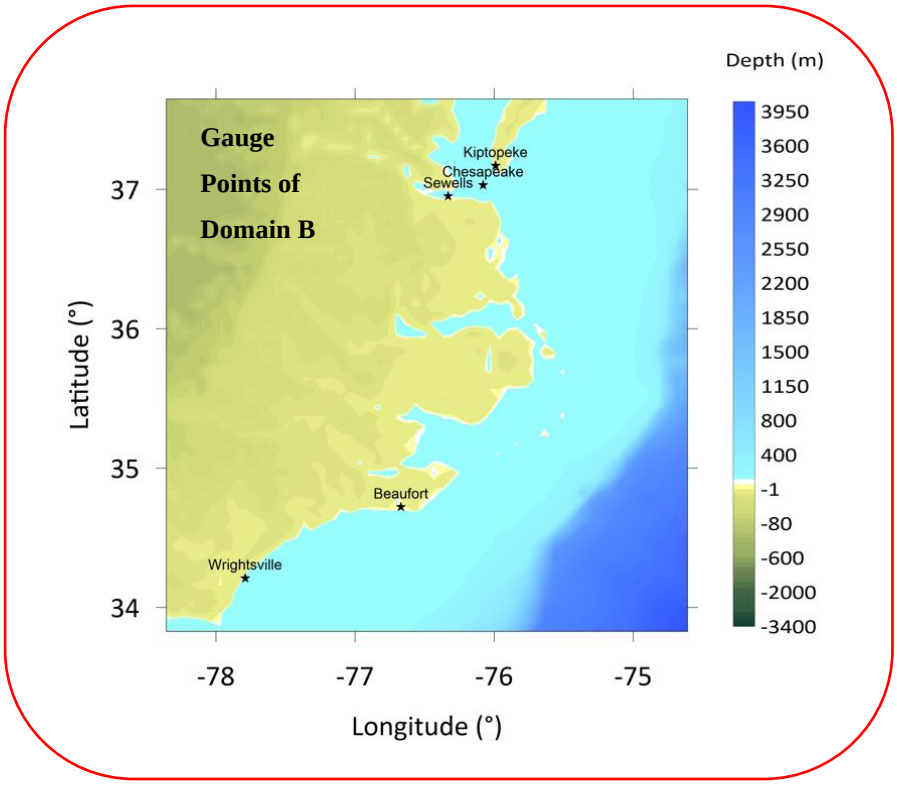


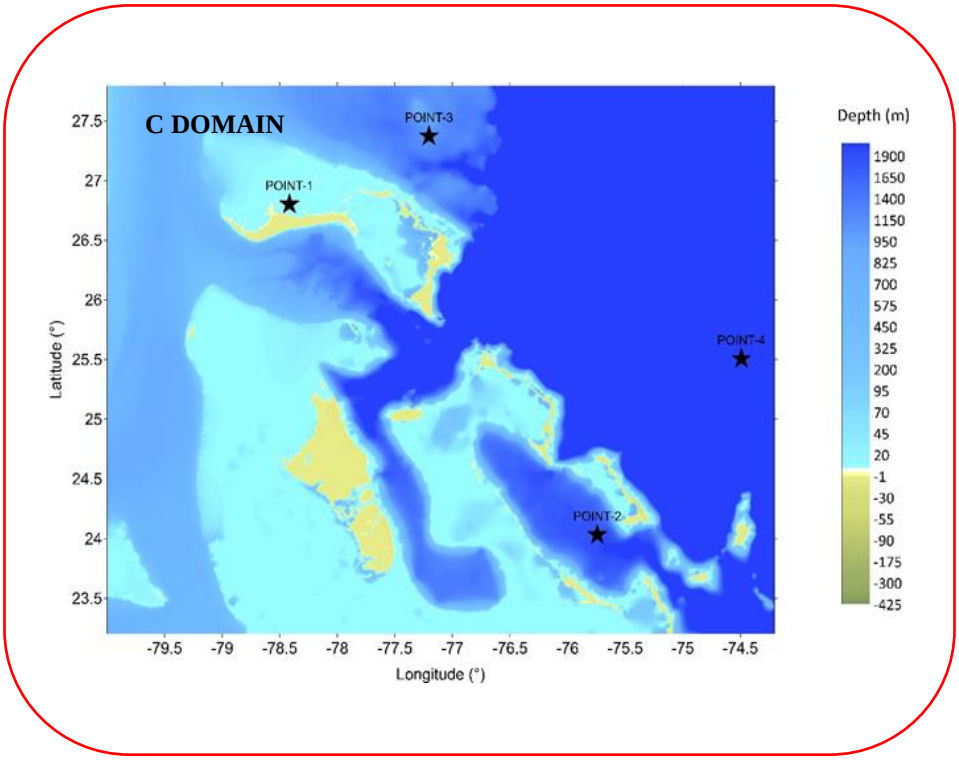


Figure 6.1. Bathymetry and gauge points of domain B and C

Table 6.1 Grid Information of the Domains

| Domains | B | C |
|---|---|---|
| Grid Dimensions | 626 rows x 570 columns | 696 rows x 552 columns |
| Xmin | -87.96666 ° Easting | -79.99791 ° Easting |
| Xmax | -46.29999° Easting | -74.20644° Easting |
| ΔX (m) | 7399.26 | 925.74 |
| Ymin | 6.03333° Northing | 23.20208° Northing |
| Ymax | 43.96666° Northing | 27.79374° Northing |
| ΔY (m) | 7399.26 | 925.74 |

### 6.1. Comparison of Input Dataset (Pressure and Wind Fields)

Three different data sources are used in Dorian simulation. Each of them has different intervals and grid resolutions. ECMWF (ERA5) data is hourly with 0.25° x 0.25° grid resolution, whereas HRES data is 6-hour intervals with 0.25° x 0.25° grid resolution, and CFSR data are both hourly and 6-hour intervals with 0.5° x 0.5° grid resolutions. The simulation is started from September 1 to September 10, 2019. There are five-gauge points taken from the NOAA observation points. Pressure and wind (Easting and Northing) data for these gauge points are compared three different data sets. Although tropical cyclone Dorian started four days before 1 September 2019, since the main pressure change can be obtained from the chosen time interval, starting the simulation before 1 September is not vital. Besides, the simulation is extended four days after the main pressure change.

### 6.1.1. Pressure Data

A comparison of three different data sets of pressure data for NOAA observation points is shown in Figure 6.2. It is seen from Figure 6.2. that the pressure data of CFSR, HRES and ERA5 are in good agreement.

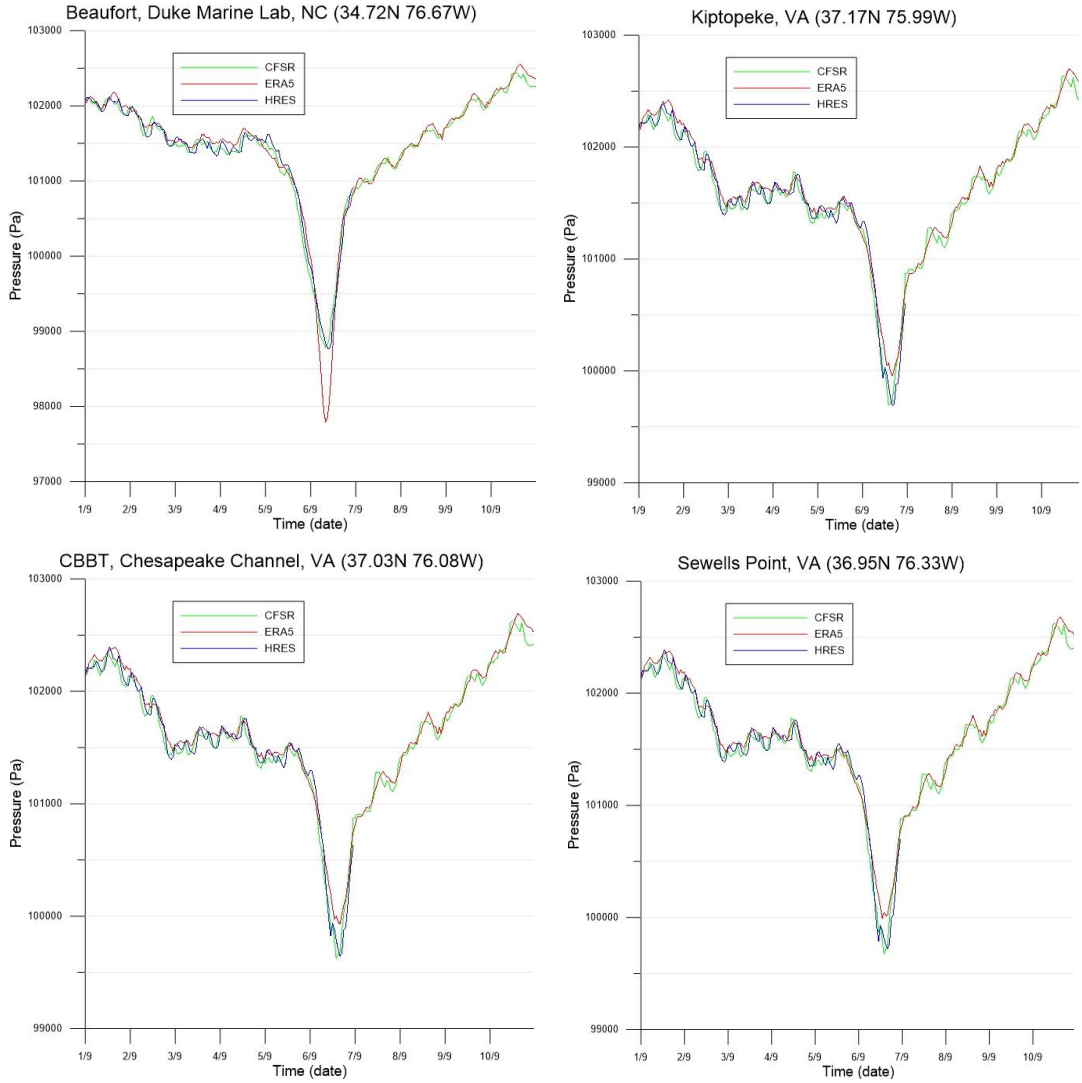

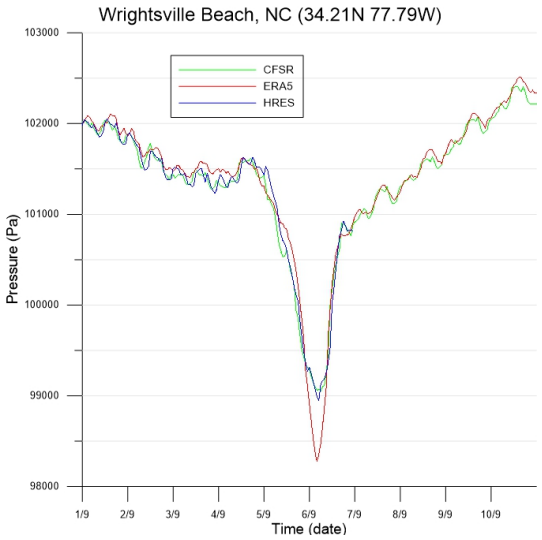


Figure 6.2. Atmospheric pressure data of CFSR, ERA5 and HRES for Beaufort, Kiptopeke, Chesapeake, Sewells and Wrightsville

A comparison of hourly and 6-hourly pressure data of CFSR for NOAA observation points is shown in Figure 6.3. It is seen from Figure 6.3. that the hourly and 6-hourly CFSR pressure data are in good agreement.

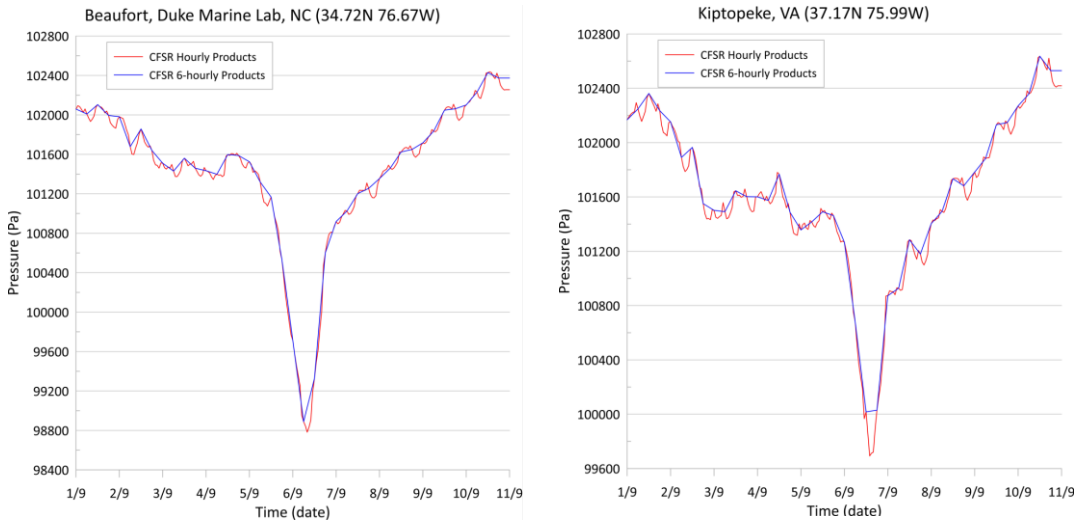

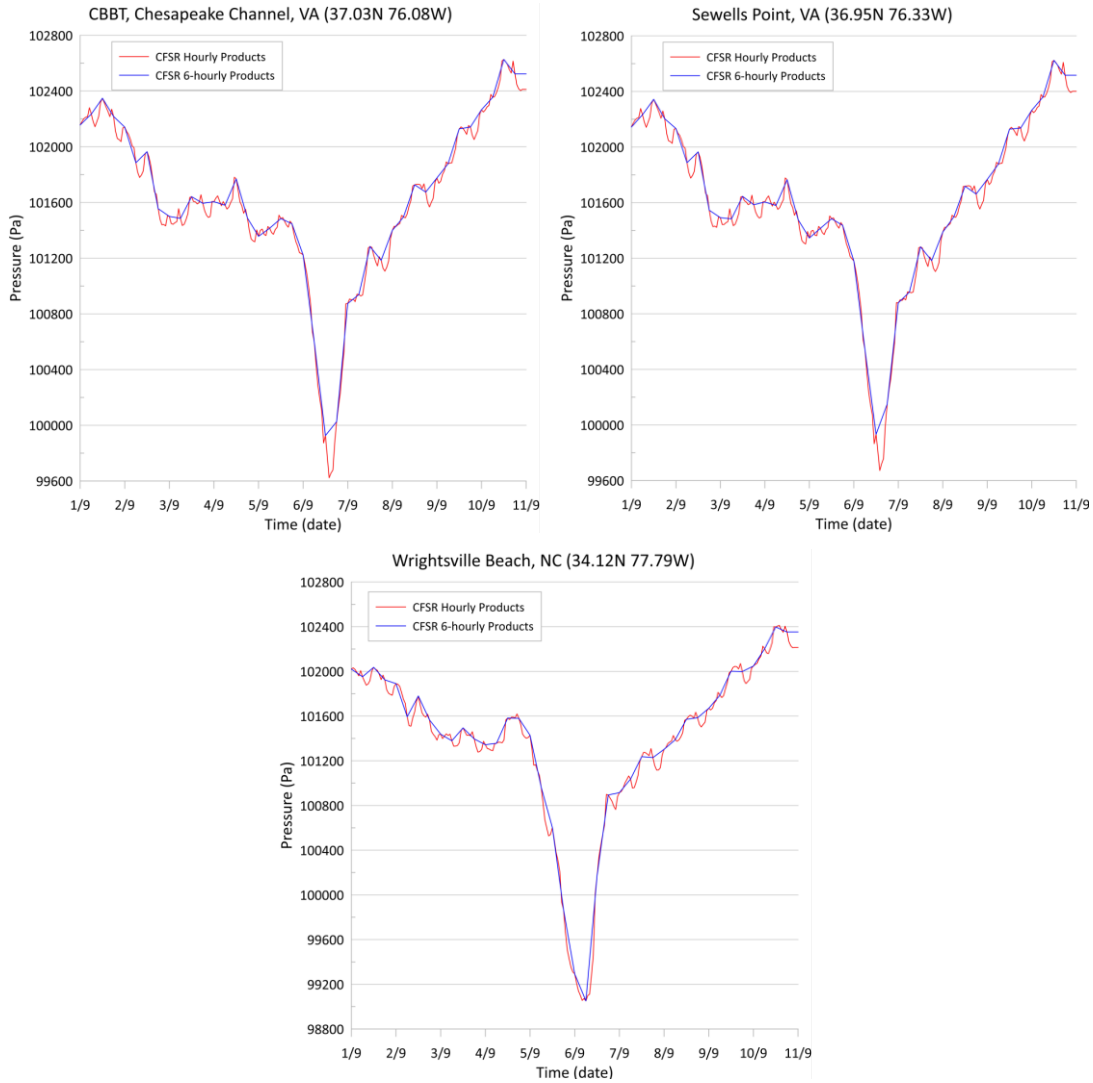


Figure 6.3. Comparison of hourly and 6-hourly CFSR atmospheric pressure data for Beaufort, Kiptopeke, Chesapeake, Sewells and Wrightsville

### 6.1.2. Wind Speed Data

A comparison of three different data sets of wind data for NOAA observation points is shown in Figure 6.4. It is seen from Figure 6.4. that the wind data of CFSR, HRES and ERA5 are in good agreement.

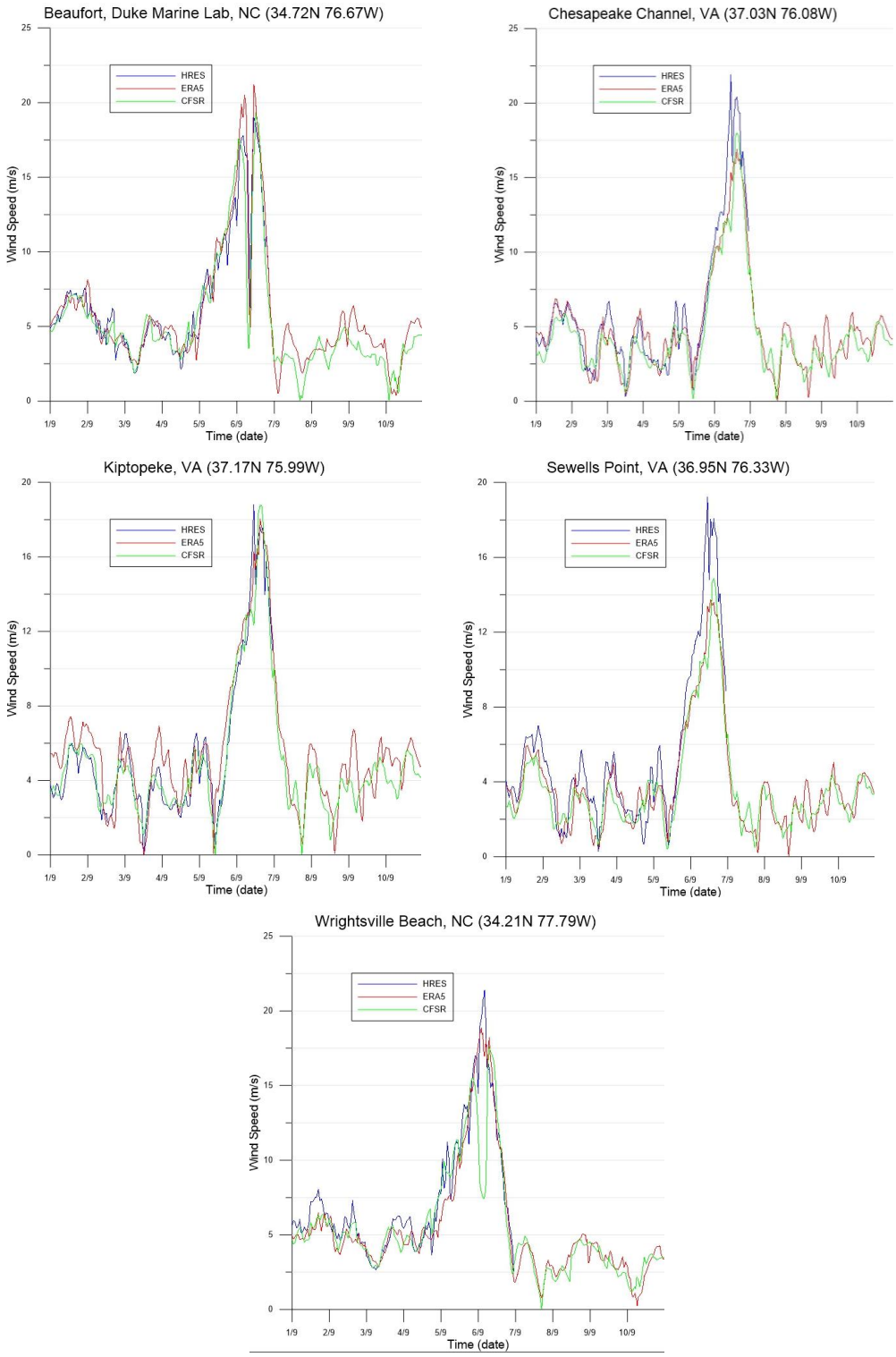


Figure 6.4. Wind data of CFSR, ERA5 and HRES for Beaufort, Kiptopeke, Chesapeake, Sewells and Wrightsville

A comparison of hourly and 6-hourly wind data of CFSR for NOAA observation points is shown in Figure 6.5. It is seen from Figure 6.5. that the hourly and 6-hourly CFSR pressure data are in good agreement.

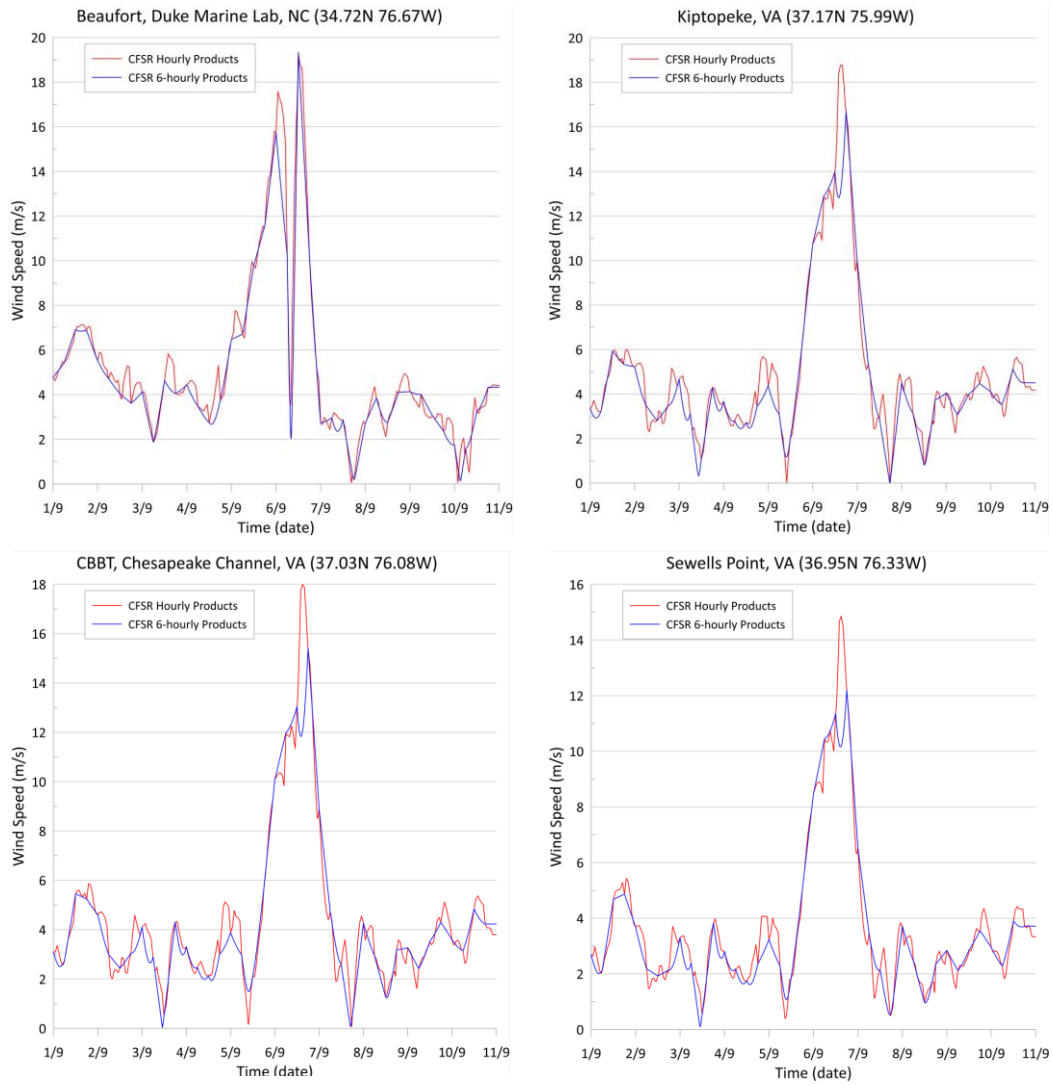

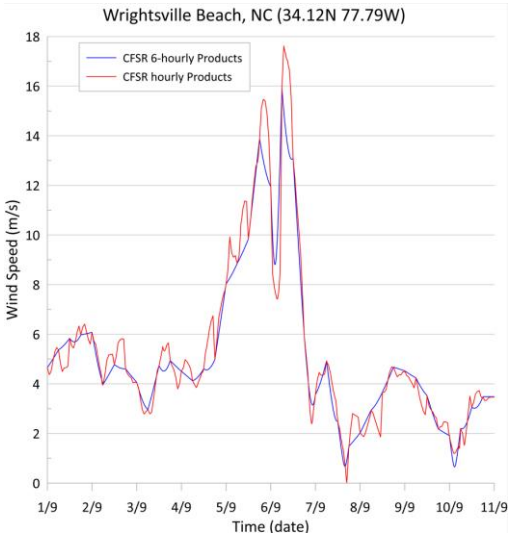


Figure 6.5. Comparison of hourly and 6-hourly CFSR wind data for Beaufort, Kiptopeke, Chesapeake, Sewells and Wrightsville

## 6.2. Comparison of Computed Water Levels

When simulation results for computed water levels for three data sets and recorded water level data from the NOAA gauge points are compared, it is clear that they are in reasonable agreement, as shown in Figure 6.6. Based on this agreement, it can be concluded that three data sets can be used for simulations from the accuracy perspective. Some differences may occur due to coastal morphology.

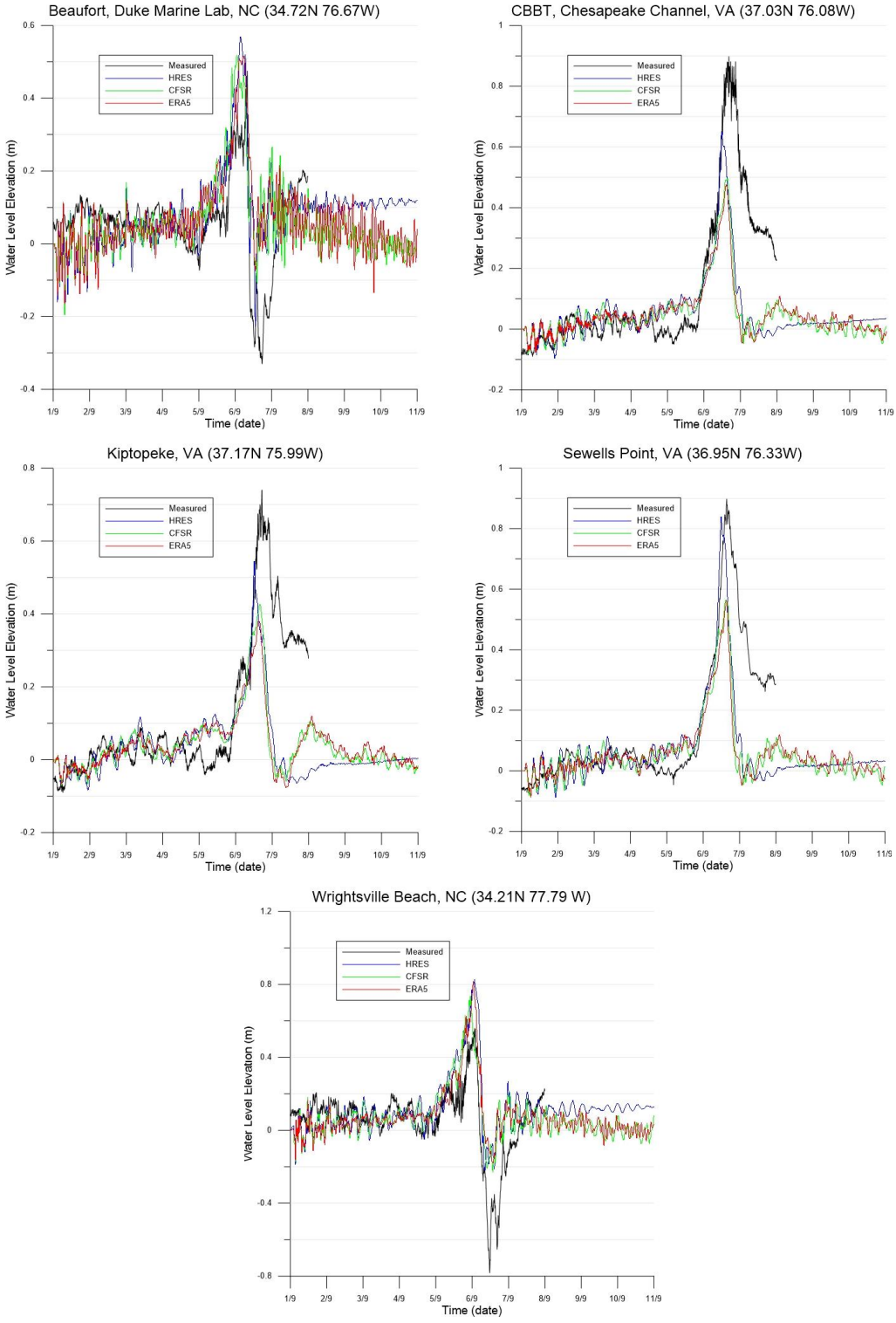


Figure 6.6. Comparison of simulated and recorded water level time-series of Beaufort, Kiptopeke, Chesapeake, Sewells, Wrightsville

A comparison of hourly and 6-hourly computed water level results of CFSR for NOAA observation points is shown in Figure 6.7. It is seen from Figure 6.7. that the hourly and 6-hourly CFSR computed water level results are in good agreement. It can be concluded that using hourly or 6-hourly CFSR data for the simulation does not make any significant difference according to the simulation performed for Dorian.

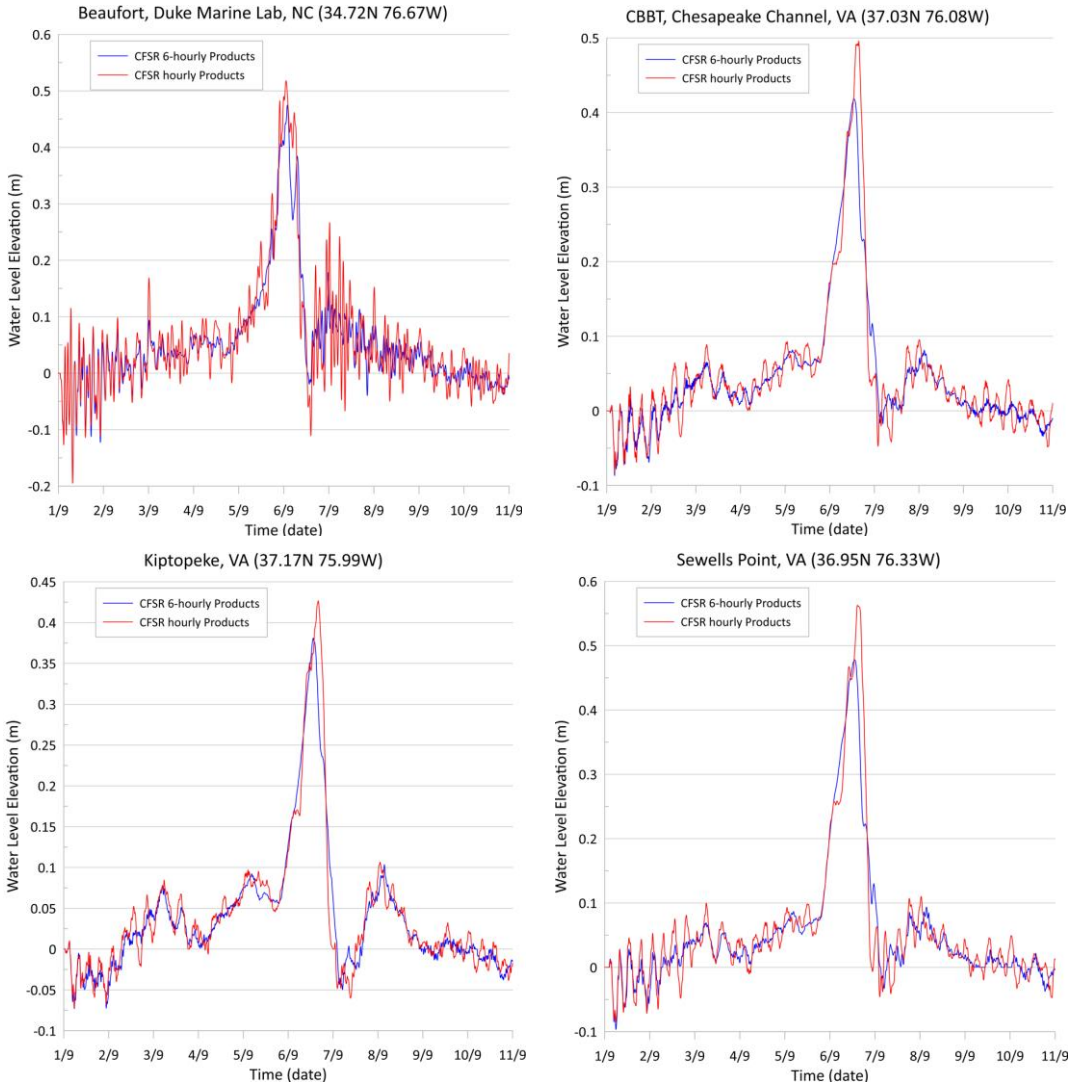

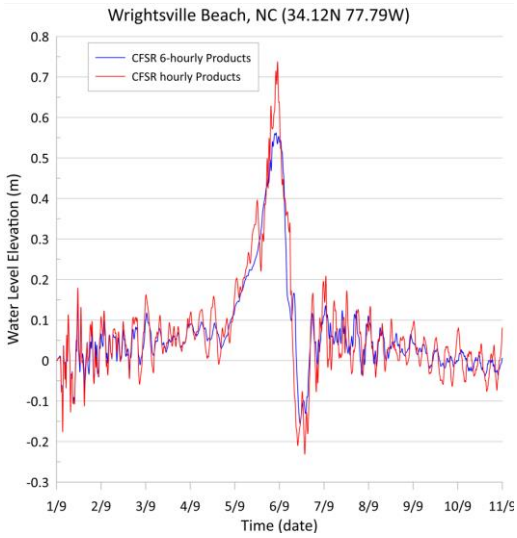


Figure 6.7. Comparison of hourly and 6-hourly CFSR computed water levels for Beaufort, Kiptopeke, Chesapeake, Sewells and Wrightsville

Table 6.2 shows the coordinates of the actual and numerical gauge stations of tropical cyclone Dorian. It also shows corresponding ECMWF and CFSR grid points and states whether they are on the sea or land. Additionally, it shows the temporal resolution of actual measurements for every station.

Table 6.3 and Table 6.4 show the coordinates of the Dorian simulation result for ECMWF and CFSR, respectively. The outputs of the simulations are the values computed at the nearest grid to the numerical gauge location.

Table 6.2 Actual and Numerical Gauge Points for Tropical Cyclone Dorian

| Stations | Actual Station | | Numerical Gauge | | | ECMWF | | | CFSR | | | Temporal Res. of Meas. |
|---|---|---|---|---|---|---|---|---|---|---|---|---|
| | Lat(°) | Long(°) | Lat(°) | Long(°) | D(m) | Lat(°) | Long(°) | Land/ Sea | Lat(°) | Long(°) | Land/ Sea | |
| Beaufort | 34.73N | 76.66W | 34.71079N | 76.66178W | 0.5 | 34.75N | 76.75W | Land | 34.5N | 283.5 | Sea | 6min. |
| Chesapeake | 37.03N | 76.08W | 37.05740N | 76.11104W | 9 | 37.0N | 76.0W | Sea | 37.0N | 284.0 | Sea | 6min. |
| Wrightsville | 34.21N | 77.79W | 34.21406N | 77.79752W | 5.8 | 34.25N | 77.75W | Sea | 34.0 | 282.0 | Land | 6min. |
| Kiptopeke | 37.17N | 75.99W | 37.16369N | 76.00920W | 8.3 | 37.25N | 76.0W | Land | 37.0 | 284.0 | Sea | 6min. |
| Sewells | 36.95N | 76.33W | 36.95834N | 76.32670W | 2 | 37.0N | 76.25W | Sea | 37.5 | 283.5 | Land | 6min. |

Table 6.3 Simulation Results of ECMWF for Tropical Cyclone Dorian

| Stations | Numerical Modelling Station | | | Actual Gauge Station | | ECMWF | | | Simulation Result (Nearest Grid) | | |
|---|---|---|---|---|---|---|---|---|---|---|---|
| | Lat(°) | Long(°) | D (m) | Lat(°) | Long(°) | Lat(°) | Long(°) | Land/ Sea | Lat(°) | Long(°) | D(m) |
| Beaufort | 34.71079N | 76.66178W | 0.5 | 34.73N | 76.66W | 34.75N | 76.75W | Land | 34,76670N | 76,56786W | -1.8 |
| Chesapeake | 37.05740N | 76.11104W | 9 | 37.03N | 76.08W | 37.0N | 76.0W | Sea | 37,10023N | 76,03435W | 4 |
| Wrightsville | 34.21406N | 77.79752W | 5.8 | 34.21N | 77.79W | 34.25N | 77.75W | Sea | 34,29847N | 77,69947W | 3 |
| Kiptopeke | 37.16369N | 76.00920W | 8.3 | 37.17N | 75.99W | 37.25N | 76.0W | Land | 37,23225N | 75,96684W | -1 |
| Sewells | 36.95834N | 76.32670W | 2 | 36.95N | 76.33W | 37.0N | 76.25W | Sea | 37,54484N | 76,25141W | 5 |

Table 6.4 Simulation Results of CFSR for Tropical Cyclone Dorian

| Stations for Dorian | Numerical Modelling Station | | | Actual Gauge Station | | CFSR | | | Simulation Result (Nearest Grid) | | |
|---|---|---|---|---|---|---|---|---|---|---|---|
| | Lat(°) | Long(°) | D (m) | Lat(°) | Long(°) | Lat(°) | Long(°) | Land/ Sea | Lat(°) | Long(°) | D(m) |
| Beaufort | 34.71079N | 283.33821E | 0.5 | 34.73N | 283.34E | 34.5N | 283.5 | Sea | 34,7667 | 283,43214 | -1.8 |
| Chesapeake | 37.05740N | 283.88895E | 9 | 37.03N | 283.92E | 37.0N | 284.0 | Sea | 37,10023 | 283,96565 | 4 |
| Wrightsville | 34.21406N | 282.20247E | 5.8 | 34.21N | 282.21E | 34.0 | 282.0 | Land | 34,29847 | 282,30053 | 3 |
| Kiptopeke | 37.16369N | 283.99079E | 8.3 | 37.17N | 284.01E | 37.0 | 284.0 | Sea | 37,23225 | 284,03316 | -1 |
| Sewells | 36.95834N | 283.67329E | 2 | 36.95N | 283.67E | 37.5 | 283.5 | Land | 37,54484 | 283,74859 | 5 |

Two types of error calculations are performed to determine the correlation between the computed and measured water level elevations. The first is the root mean square error (RMSE) and the second is the maximum value error (MAXE). While the RMSE is defined as how well it predicts the complete collection of observed data, the MAXE can be defined as the model's prediction performance for the maximum wave amplitude. The RMSE and MAXE are computed using the following equations. (IAEA- TECDOC, 2022).

$$RMSE = 100\ x\ \frac{1}{f(x_i)_{max} - f(x_i)_{min}} \sqrt{\frac{\sum(f(x)_i - y_i)^2}{n}}$$

$$MAXE = 100\ x\ \frac{|f(x_i)_{max} - y_{i_{max}}|}{f(x_i)_{max} - f(x_i)_{min}}$$

Where $f(x)_i$ values are the measured (observed) water level elevations, $y_i$ values are the computed water level elevations for every time step that has measured data. Also, $f(x_i)_{max}$ and $f(x_i)_{min}$ are the maximum and minimum measured water level elevations, respectively.

Table 6.5 shows the RMSE and MAXE results of water level elevations of five gauge stations for Dorian. As can be seen from Table 6.5, RMSE results are in acceptable range and smaller than MAXE for every station except Beaufort. It can be concluded that Dorian simulation results well capture the general trend and predict the complete collection of observed data better than the maximum water level elevations.

Table 6.5 RMSE and MAXE Results of Water Level Elevation for Dorian

| Stations | RMSE (%) | | MAXE (%) | |
|---|---|---|---|---|
| | ECMWF | CFSR | ECMWF | CFSR |
| Beaufort | 15,6 | 15,5 | 8,8 | 0,0 |
| Chesapeake | 20,3 | 19,6 | 47,0 | 53,3 |
| Kiptopeke | 21,7 | 31,9 | 48,6 | 48,6 |
| Wrightsville | 12,6 | 19,1 | 46,1 | 0,5 |
| Sewells | 18,9 | 18,1 | 37,3 | 46,8 |

The most severely devastated region, Point 1 in the Bahamas simulation result of the distribution of the maximum water surface level is shown in Figure 6.8. Grand Bahama Island's water level at Point 1 was reported to be 1.95 meters in the NHC's Hurricane Dorian report, although there is no station data for this site.

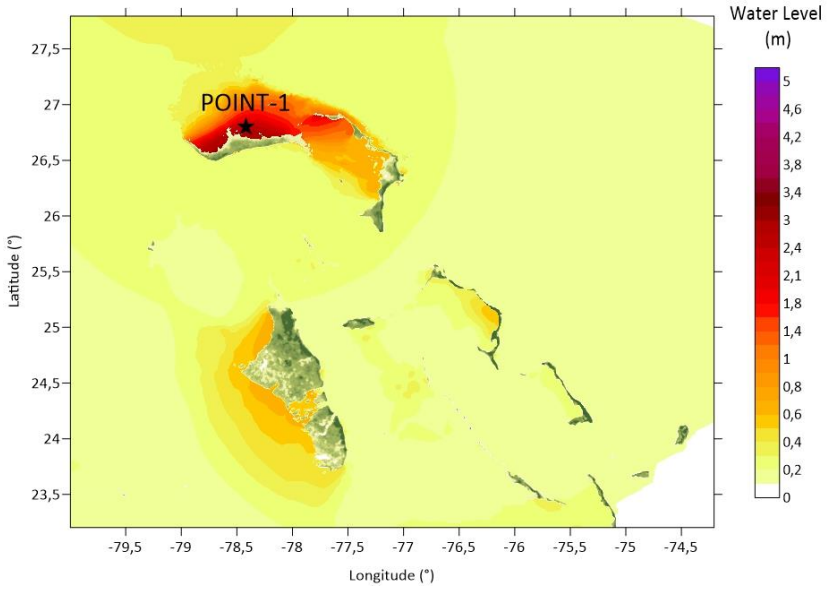


Figure 6.8. Maximum Water Level Elevation for Domain C

Additionally, Figure 6.9 provides four different locations, including Point 1 in the Bahamas. It shows that the peak sea level predicted by the model using HRES data fits well with the observed highest water level at the Grand Bahamas as 2.4 meters at Point 1. However, CFSR data does not fit well with ERA5 and HRES results for Point 1. On the other hand, Point 2, Point 3 and also Point 4 results are in a good agreement for CFSR, ERA5 and HRES data.

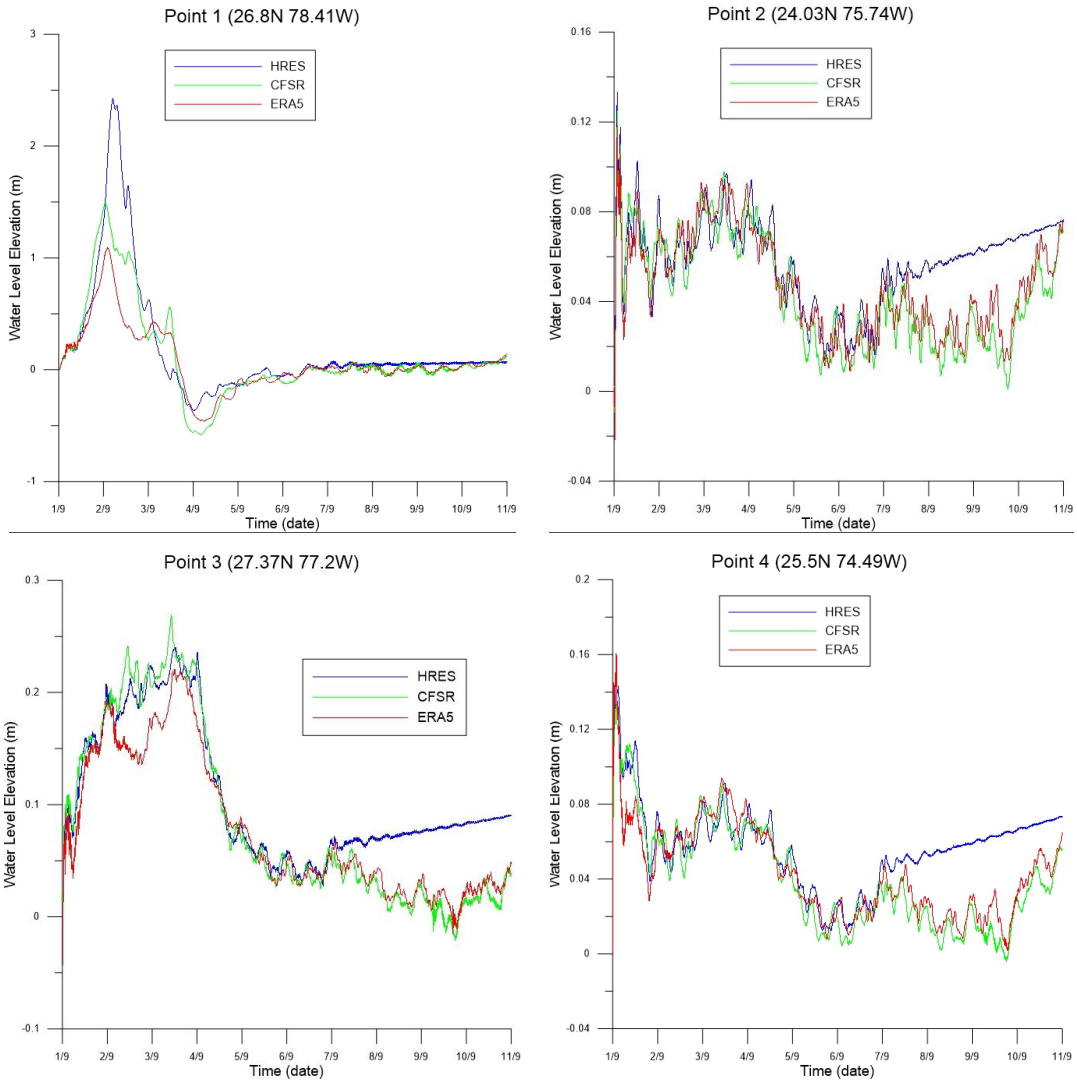


Figure 6.9. Simulated water level time-series of data source CFSR, ERA5 and HRES for Point 1, Point 2, Point 3 and Point 4

# CHAPTER 7

# APPLICATION TO MEDITERRANEAN STORMS

After the numerical modelling is applied to the tropical cyclone event Hurricane Dorian (24 August-10 September 2019) and the results are compared with the observations and measurements, recent Mediterranean storms (Medicane Trudy and Medicane Zorbas ) are modeled. The time histories of pressure and wind data of two data sources, ERA5 and CFSR are compared with each other and with actual measurements if recorded data are available. Furthermore, the time histories of the computed water level data is compared with the recorded data at tide gauge stations.

Since the impact regions of Medicane Trudy and Medicane Zorbas are southeast of Sicily island, the same nested study domains are selected for the simulations of these storms.

Bathymetry of B, C and D domains is shown in Figure 7.1. Besides, grid information for these bathymetries is shown in Table 7.1. Domain B is selected to cover central and eastern part of Mediterranean sea (Adriatic Sea and Aegean Sea), which also covers the track of these medicanes. These domains enclosed tide gauge stations of The National Tide Gauge Network of Italy and UNESCO Sea Level Station Monitoring Facility in south-eastern Sicily. Domain C and D are the nested areas, with Capo Passero and Catania being the devastated location. The bathymetry data comes from Advanced Spaceborne Thermal Emission and Reflection Radiometer (ASTER) Global Digital Elevation Map and European Marine Observation and Data Network (EMODnet). Bathymetry data is obtained by combining sea and land data taken separately from EMODnet and ASTER, respectively.

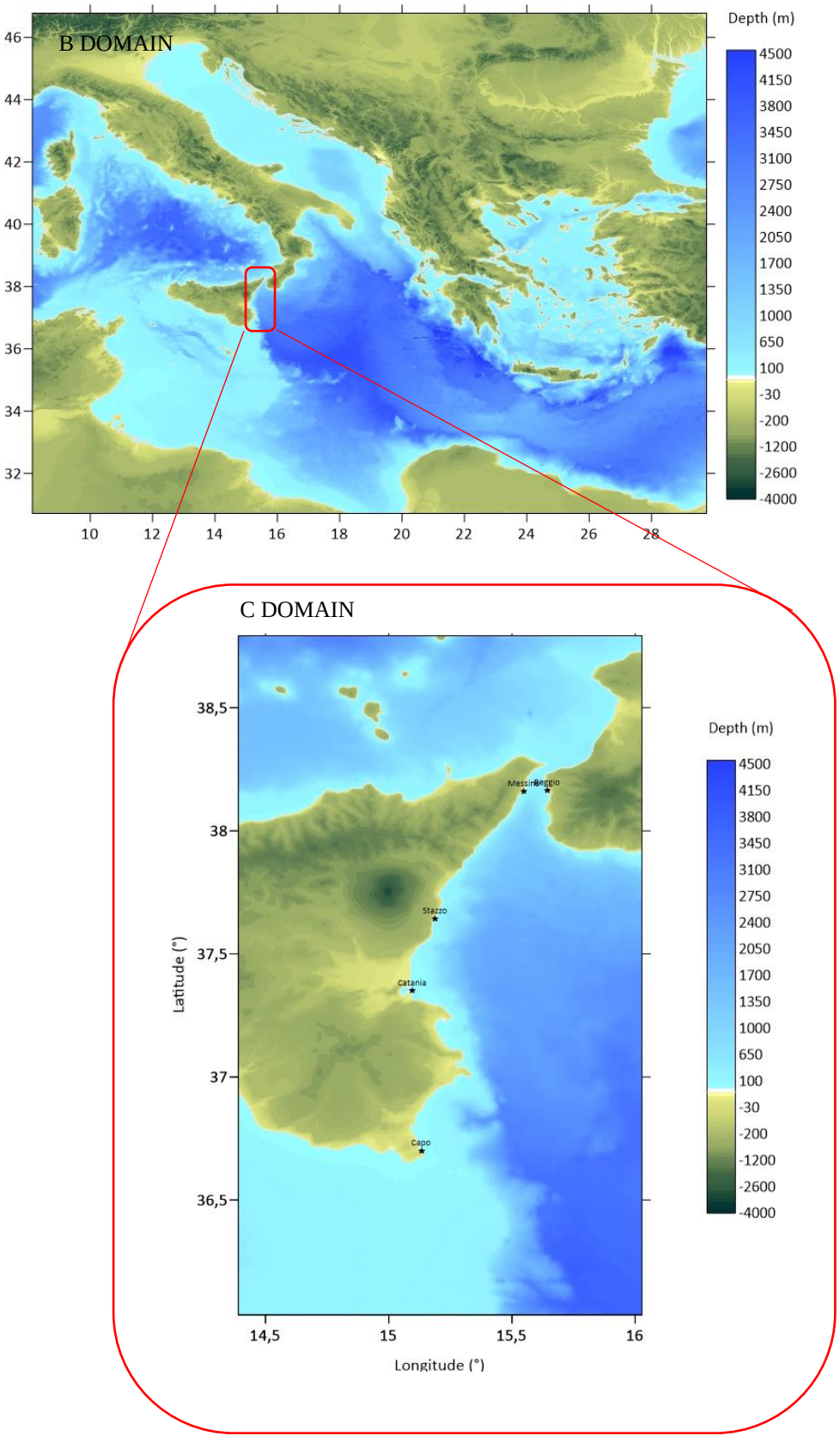
B DOMAIN
C DOMAIN
Depth (m)
4500
4150
3800
3450
3100
2750
2400
2050
1700
1350
1000
650
100
-30
-200
-1200
-2600
-4000
46
44
42
40
38
36
34
32
10
12
14
16
18
20
22
24
26
28
38,5
38
37,5
37
36,5
14,5
15
15,5
16
Latitude (°)
Longitude (°)
Messina
Reggio
Stazzo
Catania
Capo

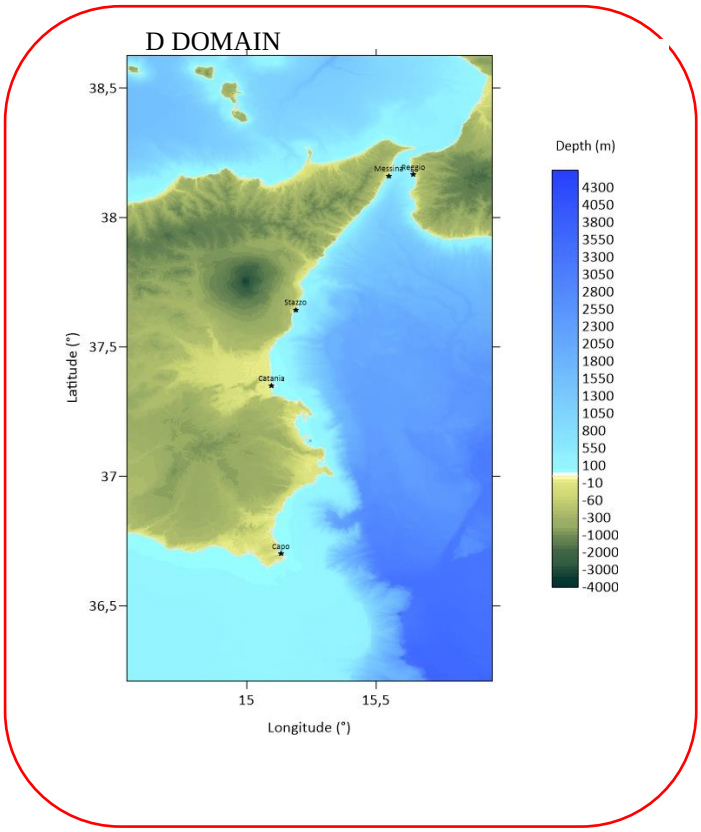


Figure 7.1. Bathymetry of B, C and D domain for Medicane Trudy and Zorbas

Table 7.1 Grid information of the Domains

| Domains | B | C | D |
|---|---|---|---|
| Grid Dimensions | 1984 rows x 2058 columns | 1022 rows x 607 columns | 5371 rows x 3138 columns |
| Xmin | 8.11447° Easting | 14.3894° Easting | 14.5368° Easting |
| Xmax | 29.76276° Easting | 16.02751° Easting | 15.9485° Easting |
| ΔX (m) | 1168.6 | 300.5 | 50 |
| Ymin | 30.71646° Northing | 36.03385° Northing | 36.2094° Northing |
| Ymax | 46.76734° Northing | 38.79228° Northing | 38.6257° Northing |
| ΔY (m) | 900 | 300.4 | 50 |

## 7.1 Medicane Trudy (11 November- 14 November 2019)

Medicane Trudy was a severe tropical cyclone that developed the low-pressure region DETLEF in the western Mediterranean on November 11, 2019, shown in Figure 7.2 (Wettergefahren- Frühwarnung, 2019). Trudy caused landfall in Algeria on November 11 (Watchers, 2019). Trudy caused much rain, with the shores of Italy recording 78 mm and the Balkans 90 mm rain on November 12 (Copernicus, 2019). During the evening of November 12, it traveled over Sicily and central Italy in a northeastern trajectory. Its eye characteristics were lost on November 13 and, on November 14, entirely lost.

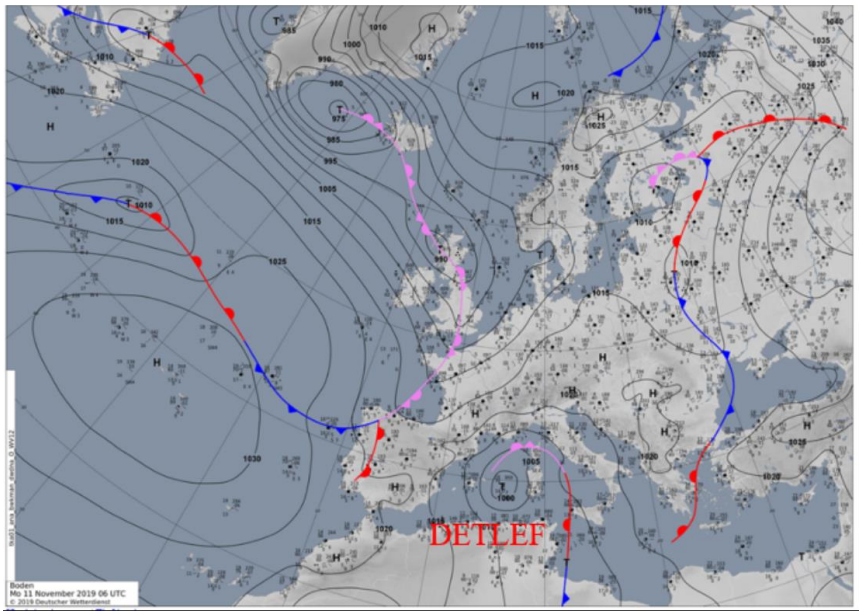


Figure 7.2. Weather analysis map of 11 November 00:00 UTC (source: Deutscher Wetterdienst, DWD)

Trudy is modelled by using NAMI DANCE in the given Figure 7.1 to compute the waves during the storm. Gauge points were selected as Catania, Messina and Reggio for the available recorded data. Pressure and wind fields are obtained from ECMWF ERA5 and CFSR data sources. ECMWF (ERA5) data is hourly with 0.25° x 0.25° grid resolution, whereas CFSR data is hourly with 0.5° x 0.5° grid resolutions. NAMI DANCE also extracted the time histories of wind fields and

pressure at the gauge points during the simulation from 11 November 2019 to 14 November 2019. It takes 4320 minutes in total and Δt (time interval) is chosen as 0.1 seconds. Pressure and wind data of ECMWF ERA5 and CFSR are compared with each other. Furthermore, the computed time histories of water level fluctuations are compared with the observations and recorded data at tide gauge stations.

### 7.1.1 Comparison of Pressure and Wind Fields

The time histories of atmospheric pressure and wind speed data of CFSR and ERA 5 at Catania are shown in Figure 7.3. Both ECMWF (ERA5) data and CFSR data are hourly. As seen in Figure 7.3, the minimum pressure is 996 mb for CFSR and ERA5 and actual pressure measurement at Catania. However, the maximum wind is 10 m/s for ERA5 and 12 m/s for CFSR data, while the measured wind speed is 50 m/s. For these outcomes, it can be claimed that both CFSR and ERA5 data miss the peak values for the wind data at Catania. The high rapid increase in wind speed data in Figure 7.3 is most probably an offset due to some measurement errors. According to Watchers (2019), the maximum wind speed reached a value of 31 m/s for Medicane Trudy.

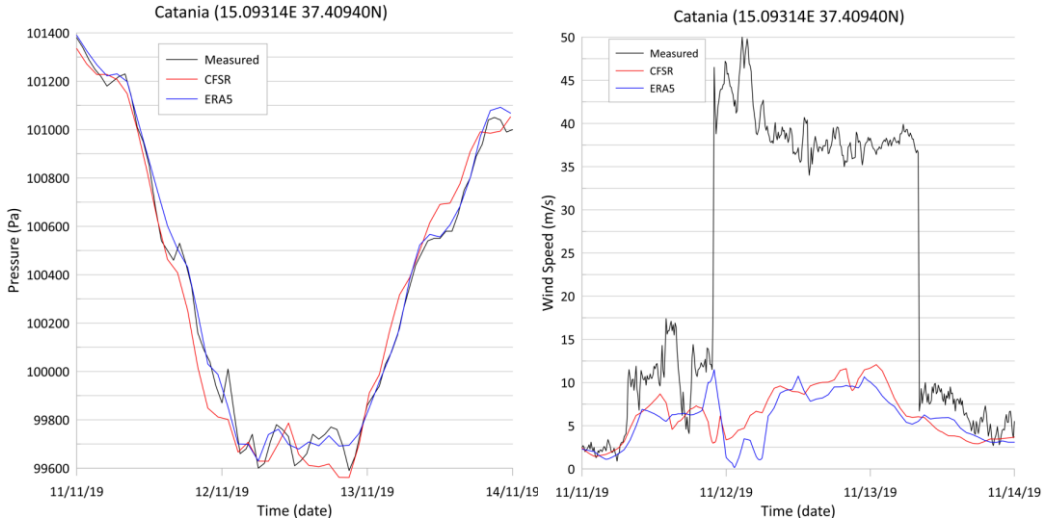


Figure 7.3. Pressure and Wind Speed for Medicane Trudy at Numerical Gauge Catania (Water Depth: 0.1412 m)

The time histories of atmospheric pressure and wind speed data of CFSR and ERA5 at Messina are shown in Figure 7.4. Both ECMWF (ERA5) data and CFSR data are hourly. As seen in Figure 7.4, the minimum pressure is 995 mb for CFSR, 994.5 mb for ERA5 and actual pressure measurement at Messina. Moreover, the maximum wind is 13 m/s for ERA5 and 16 m/s for CFSR data, while the measured wind speed is 18 m/s. For these outcomes, it can be claimed that both CFSR and ERA5 data sets agree with recorded pressure and wind data at Messina.

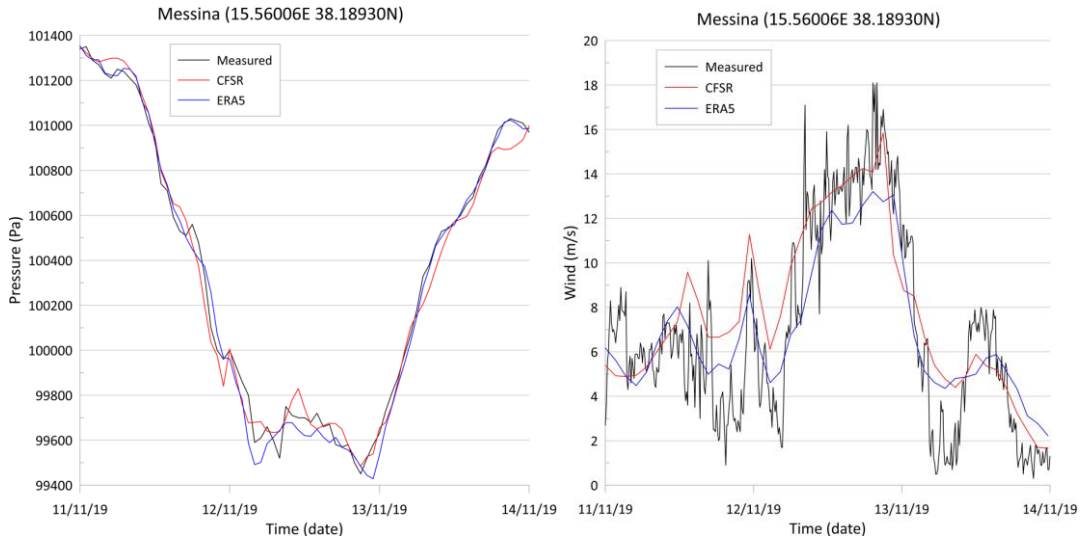


Figure 7.4. Pressure and Wind Speed for Medicane Trudy at Numerical Gauge Messina (Water Depth: 34.3329 m)

The time histories of atmospheric pressure and wind speed data of CFSR and ERA5 at Reggio are shown in Figure 7.5. Both ECMWF (ERA5) data and CFSR data are hourly. As seen in Figure 7.5, the minimum pressure is 995 mb for ERA5, CFSR and actual pressure measurement at Reggio. However, the maximum wind is 12.8 m/s for ERA5 and 15.7 m/s for CFSR data, while the measured wind speed is 9 m/s. Thereby, it can be claimed that both CFSR and ERA5 data miss the peak values for the wind data at Reggio.

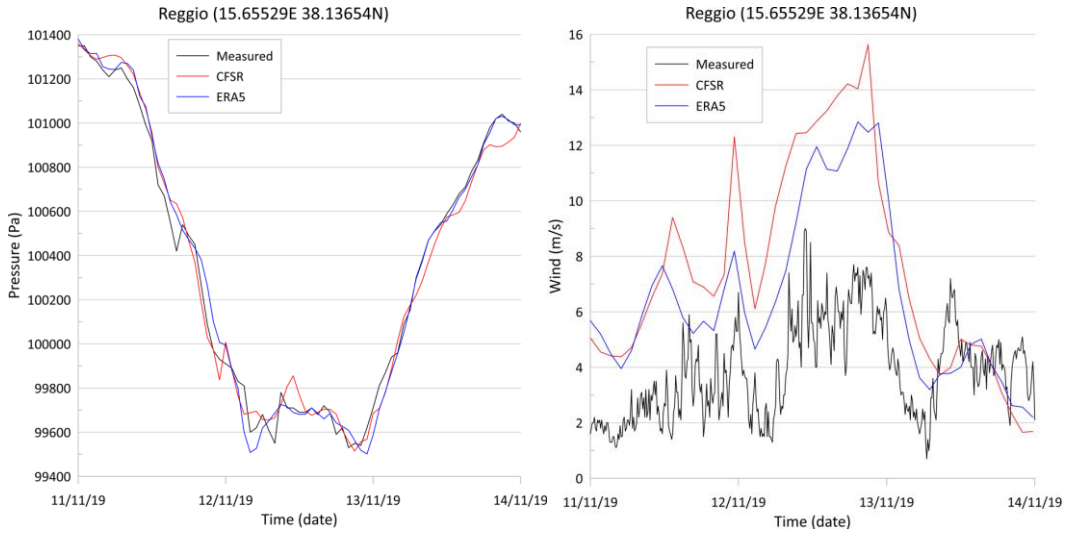


Figure 7.5. Pressure and Wind Speed for Medicane Trudy at Numerical Gauge Reggio (Water Depth: 24.2816 m)

### 7.1.2 Comparison of Computed Water Levels for Trudy

There are three available records in the tide gauge stations for tropical cyclone Trudy; Catania, Messina and Reggio. The raw sea level data obtained from tide gauge measurements have been detided by applying a band-pass filter with a cut-off period of 4 hours to remove the longer wave components. In addition, the data have been processed by a moving-average filter with a 30-min window length to obtain the surge components

Figure 7.6 shows that the computed time histories of water levels for CFSR and ERA5 data sets have similar trends at Catania. However, there is a discrepancy between the computed results and recorded water level data from The National Tide Gauge Network of Italy at Catania. Local morphological conditions can be the reason for the discrepancies.

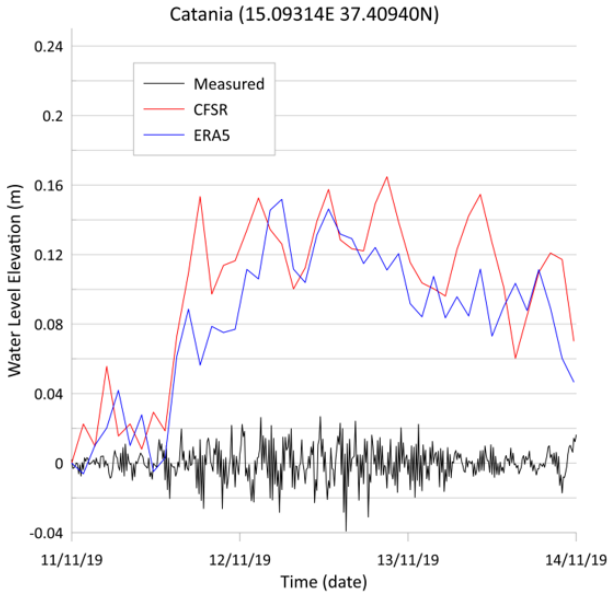


Figure 7.6. Water Level Elevation for Medicane Trudy at Numerical Gauge Catania (Water Depth: 0.1412 m)

Figure 7.7 shows that the computed time histories of water levels for CFSR and ERA5 data sets have similar trends at Messina. However, there is a discrepancy between the computed results and recorded water level data from The National Tide Gauge Network of Italy at Messina. One of the reasons for the observed discrepancies between the computed and measured water levels can be the wind drag coefficient $C_D$, which is taken as two different values for wind speed of smaller/greater than 26 m/s. It is a factor affecting the computed water levels and can be described in more detail rather than only two values for different velocity ranges. Local morphological conditions is another affecting factor which are reflected in the modelling in limited due to the spatial resolution.

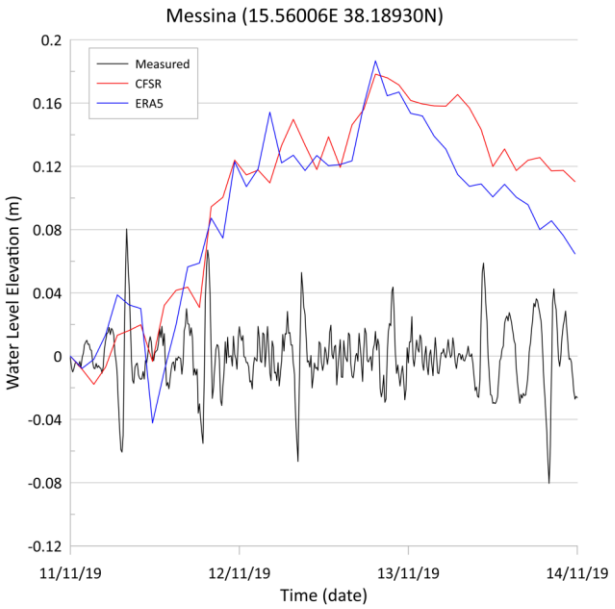


Figure 7.7. Water Level Elevation for Medicane Trudy at Numerical Gauge Messina (Water Depth: 34.3329 m)

Figure 7.8 shows that the computed time histories of water levels for CFSR and ERA5 data sets have similar trends at Reggio. However, there is a discrepancy between the computed results and recorded water level data from The National Tide Gauge Network of Italy at Reggio.

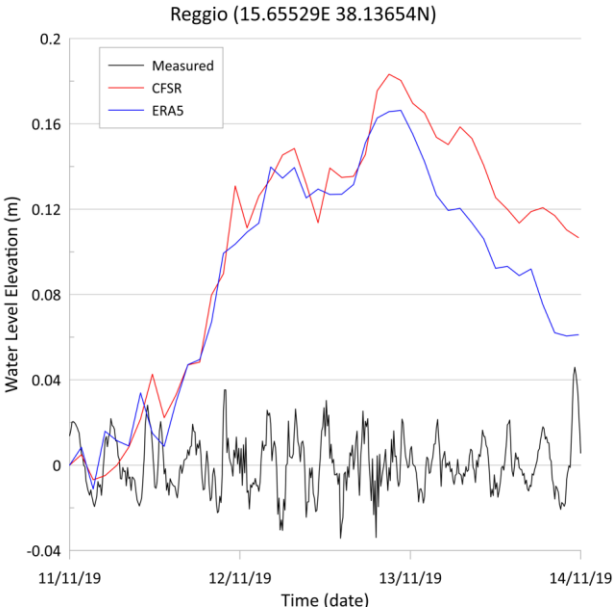

Figure 7.8. Water Level Elevation for Medicane Trudy at Numerical Gauge Reggio (Water Depth: 24.2816 m)

In summary, the inputted pressure and wind data of ERA5 and CFSR for Medicane Trudy are in agreement with the measured data at different locations. However, there are some discrepancies between the measured and computed water levels. Here it is important to note that the water level changes are small and the available data is limited.

## 7.2 Medicane Zorbas (28 September- 2 October 2018)

Tropical cyclone Zorbas formed in the eastern Mediterranean Sea and caused significant damage due to strong winds, heavy rain, and extensive floods (Floodlist, 2020; Severe-weather, 2020). Early on, Libya was the most severely hit country, and subsequently, southern Greece and Turkey (Floodlist, 2020).

Figure 7.9. Damage from Medicane Zorbas in Greece, September 2018

Tidal signals captured by Capo Passero's sensors revealed a notable surge in the water column during Medicane Zorbas. The effects of Medicane Zorbas in September 2018 in the southern Sicilian beaches, where it resulted in inland flooding and socioeconomic activity damages (Scicchitano, G. et al., 2021).

Zorbas is modelled by using NAMI DANCE in the given Figure 7.1 to compute the waves during the storm. Gauge points were selected as Capo Passero, Stazzo, Messina and Reggio for their availability. Pressure and wind fields are obtained from ECMWF ERA5 and CFSR data sources. ECMWF (ERA5) data is hourly with 0.25° x 0.25° grid resolution, whereas CFSR data is hourly with 0.5° x 0.5° grid resolutions. NAMI DANCE also extracted the time histories of wind fields and pressure at the gauge points during the simulation from 28 September 2018 to 30 September 2018. It takes 4320 minutes in total and $\Delta t$ (time interval) is chosen as 0.1 seconds. Pressure and wind data of ECMWF ERA5 and CFSR are compared with each other. Furthermore, the computed time histories of water level fluctuations are compared with the observations and recorded data at tide gauge stations.

### 7.2.1 Comparison of Pressure and Wind Fields

The time histories of atmospheric pressure and wind speed data of CFSR and ERA5 at Capo Passero are shown in Figure 7.10. Both ECMWF (ERA5) and CFSR data sets are hourly. As seen from Figure 7.10, minimum pressure is 1010.5 mb for CFSR and 1011 mb for ERA5 at Capo Passero. Furthermore, maximum wind is 9.5 m/s for ERA5 and 13.5 m/s for CFSR at the same point. It is seen from Figure 7.10 that the pressure and wind data of CFSR and ERA5 are in well agreement.

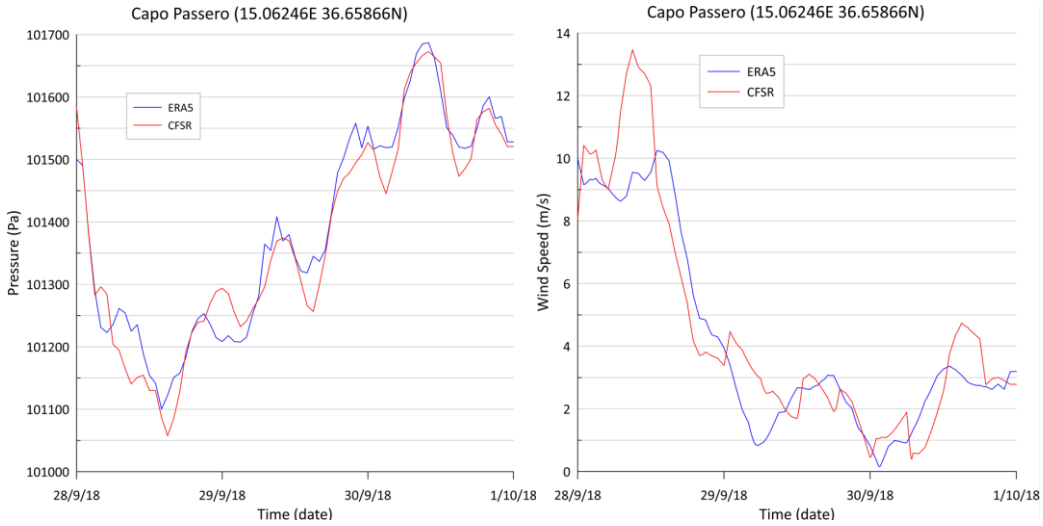


Figure 7.10. Pressure and Wind Speed for Medicane Zorbas at Numerical Gauge Capo Passero (Water Depth: 0.8367m)

The time histories of atmospheric pressure and wind speed data of CFSR and ERA5 at Stazzo are shown in Figure 7.11. Both ECMWF (ERA5) and CFSR data sets are hourly. As seen from Figure 7.11, minimum pressure is 1012.2 mb for CFSR and 1011.7 mb for ERA5. Moreover, maximum wind is 6 m/s for ERA5 and 6.5 m/s for CFSR at the same point. It is seen from Figure 7.11 that the pressure data and wind speed data of CFSR and ERA5 are in good agreement at Stazzo.

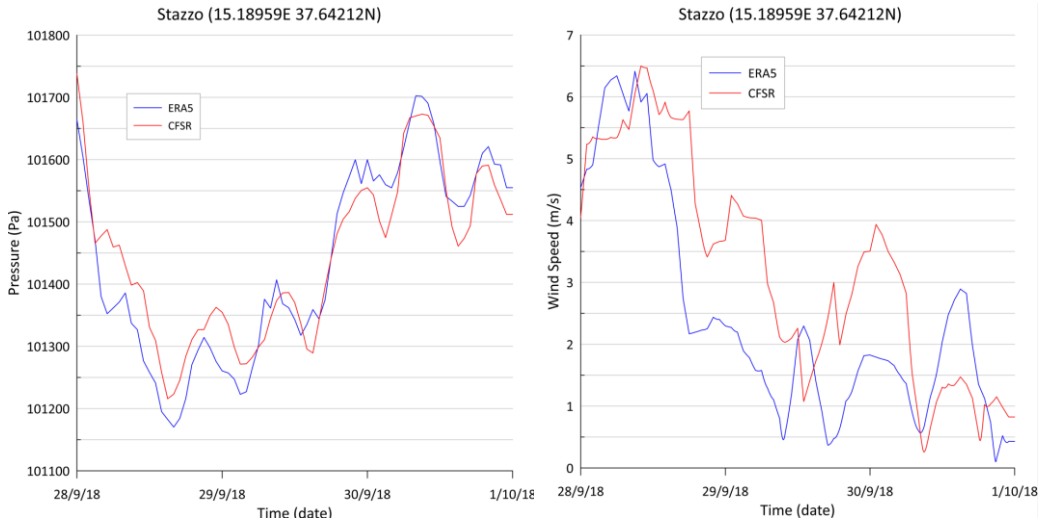


Figure 7.11. Pressure and Wind Speed for Medicane Trudy at Numerical Gauge Stazzo (Water Depth: 32.7722 m)

The time histories of atmospheric pressure and wind speed data of CFSR and ERA5 at Messina are shown in Figure 7.12. Both ECMWF (ERA5) and CFSR data sets are hourly. As seen from Figure 7.12, minimum pressure is 1012,5 mb for CFSR and 1012 mb for both ERA5 and actual pressure measurement. There is similar trend of the recorded pressure data with the data sources ERA5 and CFSR at Messina. Furthermore, maximum wind is 5 m/s for ERA5 and 6 m/s for CFSR at Mesina. It is seen from Figure 7.12 that the wind data of CFSR and ERA5 are in good agreement at Messina.

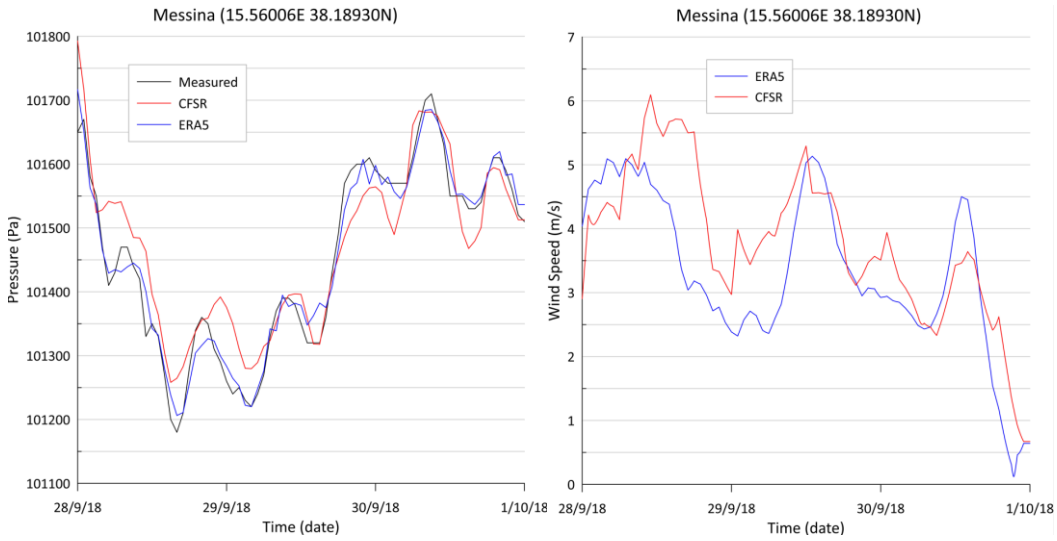


Figure 7.12. Pressure and Wind Speed for Medicane Trudy at Numerical Gauge Messina (Water Depth: 34.3329 m)

The time histories of atmospheric pressure and wind speed data of CFSR and ERA5 at Reggio are shown in Figure 7.13. Both ECMWF (ERA5) and CFSR data sets are hourly data is hourly. As seen from Figure 7.13, minimum pressure is 1012.5 mb for CFSR and 1012 mb for both ERA5 and actual pressure measurement. There is similar trend of the recorded pressure data with the data sources ERA5 and CFSR at Reggio. Moreover, maximum wind is 5.2 m/s for ERA5 and 5.7 m/s for CFSR at the same point. It is seen from Figure 7.13 that the wind data of CFSR and ERA5 are in good agreement at Reggio.

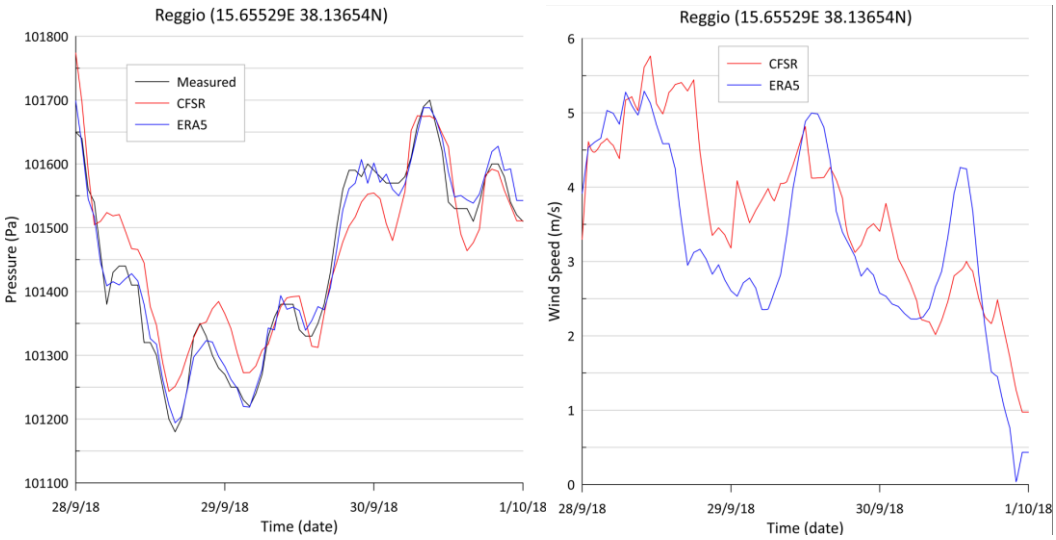


Figure 7.13. Pressure and Wind Speed for Medicane Trudy at Numerical Gauge Reggio (Water Depth: 24.2816 m)

### 7.2.2 Comparison of Computed Water Levels for Zorbas

There are three available records in the tide gauge stations for tropical cyclone Zorbas; Capo Passero, Messina and Reggio. The raw sea level data obtained from tide gauge measurements have been detided by applying a band-pass filter with a cut-off period of 4 hours to remove the longer wave components. In addition, the data have been processed by a moving-average filter with a 30-min window length to obtain the surge components

Figure 7.14 shows the computed time histories of the water level at Capo Passero using CFSR and ERA5 data with similar trends. Furthermore, those have a good agreement with the recorded water level data from the UNESCO tide gauge station at Capo Passero.

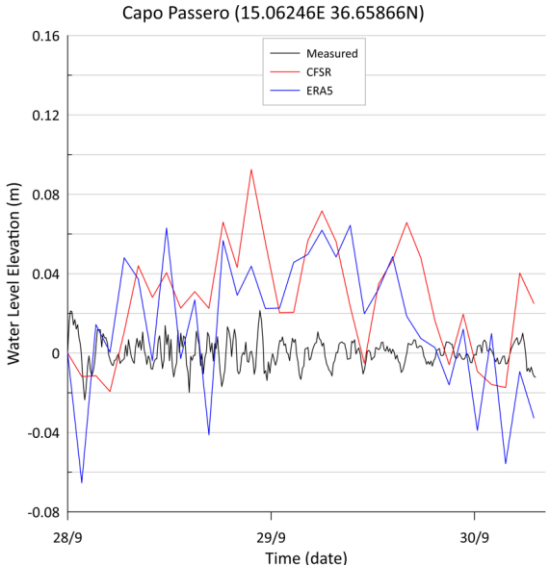


Figure 7.14. Water Level Elevation for Medicane Zorbas at Numerical Gauge Capo Passero (Water Depth: 0.8367 m)

Figure 7.15 shows that the computed time histories of water levels for CFSR and ERA5 data sets have similar trends at Messina. However, there is a discrepancy between the computed results and recorded water level data from UNESCO tide gauge station at Messina.

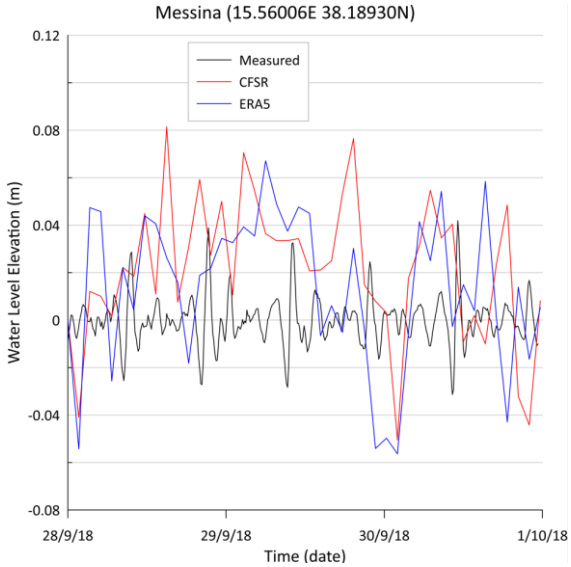


Figure 7.15. Water Level Elevation for Medicane Zorbas at Numerical Gauge Messina (Water Depth: 34.3329 m)

Figure 7.16 shows that the computed time histories of water levels for CFSR and ERA5 data sets have similar trends at Reggio. However, there is a discrepancy between the computed results and recorded water level data from UNESCO tide gauge station at Reggio.

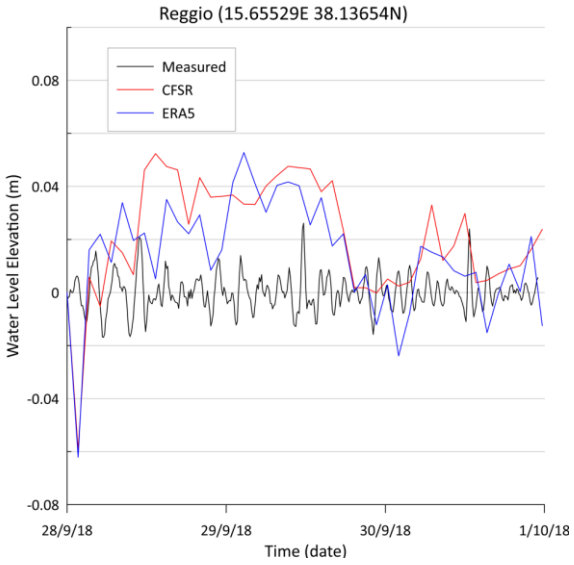


Figure 7.16. Water Level Elevation for Medicane Zorbas at Numerical Gauge Reggio (Water Depth: 24.2816 m)

For the summary of the discussion of the results: the simulation result shows that Medicane Zorbas for ERA5 and CFSR pressure and wind data have similar trends. Furthermore, their computed water levels also follow similar trends with an acceptable discrepancy. Local morphological conditions are again one of the reasons of discrepancies. It should be noted that amplitudes of computed and measured water levels are small, which may cause large errors.

Table 7.2 shows the coordinates of actual and numerical gauge stations of tropical cyclone Trudy and Zorbas. It also shows corresponding ECMWF and CFSR grid points and states whether they are on the sea or land. Additionally, it shows the temporal resolution of actual measurements for every station with its corresponding Medicane.

Table 7.2 Actual and Numerical Gauge Points for Tropical Cyclone Trudy and Zorbas

| Stations for Zorbas and Trudy | Numerical Modelling Station | | | Actual Gauge Station | | ECMWF | | | CFSR | | | Temporal Res. of Meas. | |
|---|---|---|---|---|---|---|---|---|---|---|---|---|---|
| | Lat (°) | Long (°) | D (m) | Lat (°) | Long (°) | Lat (°) | Long (°) | Land/ Sea | Lat (°) | Long (°) | Land / Sea | Trudy | Zorbas |
| Capo Passero | 36.65866 N | 15.06246 E | 0.84 | 36.666 30N | 15.11233E | 36.75 N | 15.0 E | Land | 36.5 N | 15.0 E | Sea | - | 1min |
| Messina | 38.18930 N | 15.56006 E | 343.33 | 38.196 31N | 15.56351E | 38.25 N | 15.5 E | Land | 38.0 N | 15.5 E | Sea | 10 min | 1min |
| Reggio | 38.13654 N | 15.65529 E | 242.82 | 38.121 71N | 15.64891E | 38.25 N | 15.75 E | Land | 38.0 N | 15.5 E | Sea | 10 min | 1min |
| Catania | 37.40940 N | 15.09314 E | 0.14 | 37.498 08N | 15.09382E | 37.5 N | 15.0 E | Land | 37.5 N | 15.0 E | Land | 10 min | - |

Table 7.3 shows the coordinates of the Trudy and Zorbas simulation results for ECMWF and CFSR. The outputs of the simulations are the values computed at the nearest grid to the numerical gauge location.

Table 7.3 Simulation Results of ECMWF for Tropical Cyclone Trudy and Zorbas

| Stations | Actual Station | | Location | Numerical Gauge | | | ECMWF | | | CFSR | | | Simulation Result (Nearest Grid) | | |
|---|---|---|---|---|---|---|---|---|---|---|---|---|---|---|---|
| | Lat(°) | Long(°) | | Lat(°) | Long(°) | D(m) | Lat (°) | Long (°) | Land/ Sea | Lat (°) | Long (°) | Land/ Sea | Lat(°) | Long(°) | D(m) |
| Capo Passero | 36.66630 N | 15.11233 E | Portopalo di C.Passero | 36.65866 N | 15.06246 E | 0.8367 | 36.75N | 15.0E | Land | 36.5N | 15.0E | Sea | 36.65888 N | 15.06281 E | 0.48 |
| Messina | 38.19631 N | 15.56351 E | Naval Command | 38.18930 N | 15.56006 E | 343.329 | 38.25N | 15.5E | Land | 38.0N | 15.5E | Sea | 38.18865 N | 15.56051 E | 1.8 |
| Reggio | 38.12171 N | 15.64891 E | Hydrofoil berthing | 38.13654 N | 15.65529 E | 242.816 | 38.25N | 15.75E | Land | 38.0N | 15.5E | Sea | 38.13678 N | 15.65588 E | 11 |
| Catania | 37.49808 N | 15.09382 E | Commercial seaport | 37.40940 N | 15.09314 E | 0.1412 | 37.5N | 15.0E | Land | 37.5N | 15.0E | Land | 37.40995 N | 15.09341 E | 0.14 |

Two types of error calculations are performed to determine the correlation between the computed and measured water level elevations for Medicane Trudy and Zorbas. The first is the root mean square error (RMSE) and the second is the maximum value error (MAXE) and their equations are mentioned in tropical cyclone Dorian section.

Table 7.4. shows the RMSE and MAXE results of water level elevations of three gauge stations for Medicane Trudy. As can be seen from Table 7.4, both the RMSE and MAXE results are higher than expected. The major causes of the errors are the locations of the tide gauges and the local morphological conditions. The tide gauges are located in the protected areas such as ports and harbors which are not present in the numerical model. Ten minutes temporal resolution of actual measurements for every station in Trudy may cause these unexpected errors. Trudy is a moderate scale cyclone event and the temporal and spatial resolution of pressure and wind speed data seem uncapable of regenerating the observed water levels in simulations for such an event.

Table 7.4 RMSE and MAXE Results of Water Level Elevation Trudy

| Stations | RMSE (%) | | MAXE (%) | |
|---|---|---|---|---|
| | ECMWF | CFSR | ECMWF | CFSR |
| Catania | 52,1 | 60,5 | 77,0 | 92,4 |
| Messina | 67,9 | 74,5 | 60,4 | 72,9 |
| Reggio | 131,3 | 148,4 | 97,3 | 117,0 |

Table 7.5. shows the RMSE and MAXE results of water level elevations of three gauge stations for Medicane Zorbas. As can be seen from Table 7.5, the MAXE results are smaller than the RMSE for every station. It can be concluded that Zorbas simulation results predict the maximum water level elevations better than the complete collection of observed data. Similar reasons to the Medicane Trudy for high errors in Medicane Zorbas can also be stated here.

Table 7.5 RMSE and MAXE Results of Water Level Elevation Zorbas

| Stations | RMSE (%) | | MAXE (%) | |
|---|---|---|---|---|
| | ECMWF | CFSR | ECMWF | CFSR |
| Capo Passero | 93,2 | 95,1 | 57,5 | 38,7 |
| Messina | 48,3 | 50,9 | 31,5 | 60,3 |
| Reggio | 64,6 | 69,8 | 47,1 | 41,5 |

# CHAPTER 8

# SUMMARY AND CONCLUSION

Tropical cyclones are the one of the greatest risks to life and property. They composed of a variety of hazards, including storm surge, floods, and extremely strong winds. Mediterranean hurricanes are the cyclones with tropical characteristics and known as medicanes which occasionally develop in the Mediterranean Sea. The Mediterranean coasts are becoming more vulnerable to coastal erosion, particularly as a result of the more frequent and powerful Medicanes. They have a significant potential for damage like storm surges and tsunamis, consequently accurate simulations of their evolution in climate scenarios are essential for a sufficient response to climate change

The selected tropical cyclones and storm events in the Mediterranean Sea are modelled and results are compared with different data sets and also actual measurements from tide gauge stations. The numerical model is built up on the tsunami numerical model NAMI DANCE GPU version and therefore, has the capability of computing the spatial and temporal distribution of water levels throughout the study domain. As the case studies firstly, the numerical modelling is applied to the tropical cyclone event Dorian (28 August-10 September 2019) and the results are compared with the observations and measurements. ECMWF (ERA5), HRES and CFSR are hourly data sets. It is noticeable that models often follow a similar pattern. Pressure and wind (Northing, Easting) data for these gauge points are compared and the results are in reasonable agreement. The computed water levels for three data sets and recorded water level data from the NOAA gauge points are compared, it is clear they are also in reasonable agreement. It can be said that Dorian simulations results have a similar trend with actual measurements since the RMSE results are in an acceptable range. However, the maximum points have some differences. Furthermore, the most damaged region

Bahamas' simulated water level elevation was simulated as 2.4 and the observation is 1.95 meters. This slight difference can emerge from the fact that NAMI DANCE (which is based on nonlinear shallow water equations) solely computes long waves including infragravity waves. In addition, some differences may occur due to coastal morphology.

After the NAMI DANCE verification for Dorian, new simulations are performed using the data of Mediterranean storms, Medicane Trudy (November 2019) and Medicane Zorbas (September 2018) in the nested domains B, C and D, which are focused on the coast of Southeastern Sicily. This region is impacted by both events. Catania is selected as one of the main gauge points for the Medicane Trudy simulation because of the available measurement (pressure, wind and water level) data. It is seen that if there are pressure and wind measurements, CFSR and ECMWF (ERA5) pressure and wind data sets fit well. When the computed results are compared with each other, there is an acceptable discrepancy between the computed results and recorded water level data from The National Tide Gauge Network of Italy.

Capo Passero is selected as one of the main gauge points for the Medicane Zorbas simulation because of the available measurement (pressure, wind and water level) data. It is seen that if there are pressure and wind measurements, the CFSR and ECMWF wind and pressure data sets fit well. When the computed results are compared with each other, there is an acceptable discrepancy between the computed results and recorded water level data from UNESCO tide gauge stations. Small amplitudes of computed and measured water levels may cause these discrepancies. It should be noted here that the local morphological and bathymetrical conditions, which could not be included in the input grid of simulations due to spatial resolution and available bathymetry/topography data are the major affecting factors of the differences for both cases.

There can be several reasons for high values of the RMSE and MAXE in Medicane Trudy and Zorbas. The first reason is related with the uncertainties in measured

data, i.e., the temporal resolution of measured data is ten minutes in some locations. The second reason is the resolution of bathymetry/topography data. Due to the resolution of bathymetry data, the actual locations of the stations and local morphological conditions can not be reflected in the model. The tide gauges are located in the protected areas such as ports and harbors which are not present in the numerical model. Finally, the temporal and spatial resolution of wind and pressure input data can cause additional errors.

The main experience gained from this study is that there is quite well agreement between the temporal change of pressure and wind field data of CFSR and ECMWF. Furthermore, they are also in good agreement with the corresponding measured data. The computed sea level data show a similar trend to the measured sea level data. However, some discrepancies may come from the small amplitudes of the water level change especially for the medicanes. It is also observed that the pressure is more effective on the computed water level when compared to the wind effect. Wind drag coefficient and its functional representation in the computations is another parameter to be considered for better simulation results.

As the summary and main objectives of the study: two data sets of different resources are compared with each other, obtained agreement on the pressure and wind speed of two data sources, tropical cyclones are simulated and computed water level data are compared with observations which have a good agreement.

High-resolution spatial and temporal data are vital for future studies to ensure more better simulation results. For this study, hourly data sets are used for wind and pressure inputs and this is one of the main limitations of this study. Because as seen from the outputs, simulation results can not capture smaller events and sometimes miss the peak points. For instance, minute sea level datasets can be more useful than hourly data in acquiring accurate results. Furthermore, limited number of measurement stations is another limitation and there should be more comparison points to reach proper conclusions. Additionally, more cyclone events including other data sources preferably from regional improved models such as Japan

Meteorological Agency (JMA) for a case in that area can be modelled as future studies.

## REFERENCES


Aster Global Digital Elevation Map. (2022). Retrieved from https://asterweb.jpl.nasa.gov/gdem.asp

Atmospheric reanalysis data. (2022). Retrieved from https://rda.ucar.edu

Climate Data Guide. Retrieved from https://climatedataguide.ucar.edu/climate-data/climate-forecast-system-reanalysis-cfsr

Copernicus Climate Data Store. (2022). Retrieved from https://cds.climate.copernicus.eu/

Dogan, G. G., Pelinovsky, E., Zaytsev, A., Metin, A. D., Ozyurt Tarakcioglu, G., Yalciner, A. C., ... & Didenkulova, I. (2021). Long wave generation and coastal amplification due to propagating atmospheric pressure disturbances. Natural Hazards, 106(2), 1195-1221.

ECMWF About home. Retrieved from https://www.ecmwf.int/en/about

ERA5. Retrieved from https://www.ecmwf.int/en/forecasts/datasets/reanalysis-datasets/era5

European Commission - Sea Levels Database. (2022). Retrieved from https://webcritech.jrc.ec.europa.eu/SeaLevelsDb

European Marine Observation and Data Network (EMODnet). (2022). Retrieved from https://www.emodnet-bathymetry.eu/

Flood List (2018). Greece – 3 Missing in 'Storm Zorba' Floods- Retrieved from https://floodlist.com/europe/greece-medicane-zorba-september-2018

Fritz, H. M., Blount, C. D., Albusaidi, F. B., & Al-Harthy, A. H. M. (2010). Cyclone Gonu storm surge in Oman. Estuarine, Coastal and Shelf Science, 86(1), 102-106.

General Bathymetric Chart of the Oceans. (2022). GEBCO - Gridded bathymetry data (general bathymetric chart of the oceans). Retrieved from https://www.gebco.net/

Gutiérrez-Fernández, J., González-Alemán, J. J., de la Vara, A., Cabos, W., Sein, D. V., & Gaertner, M. Á. (2021). Impact of ocean–atmosphere coupling on future projection of Medicanes in the Mediterranean sea. International Journal of Climatology, 41(4), 2226-2238.

IAEA- TECDOC (2022). In Benchmark analysis of numerical models for tsunami simulation, International Atomic Energy Agency IAEA-TECDOC-1973, pp. 6–7. https://www.iaea.org/publications/14923/benchmark-analysis-of-numerical-models-for-tsunami-simulation

Medicane "trudy" (Detlef, Bernardo) makes landfall in Algeria. (2022, March 25). Retrieved from https://watchers.news/2019/11/12/medicane/

Miglietta, M. M. (2019). Mediterranean tropical-like cyclones (Medicanes). Atmosphere, 10(4), 206.

Moon, I. J., Kim, S. H., & Chan, J. C. (2019). Climate change and tropical cyclone trend. Nature, 570(7759), E3-E5.

NATIONAL HURRICANE CENTER. (2020, April). Tropical Cyclone Report Hurricane Dorian ((AL052019)). https://www.nhc.noaa.gov/data/tcr/AL052019_Dorian.pdf

Nissen, K. M., Leckebusch, G. C., Pinto, J. G., & Ulbrich, U. (2014). Mediterranean cyclones and windstorms in a changing climate. Regional environmental change, 14(5), 1873-1890.

NOAA National Weather Service. (2011, April 01). Climate forecast system version 2 (CFSV2) operational forecasts. Retrieved from https://www.ncei.noaa.gov/access/metadata/landing-page/bin/iso?id=gov.noaa.ncdc%3AC00877

Pytharoulis, I. (2018). Analysis of a Mediterranean tropical-like cyclone and its sensitivity to the sea surface temperatures. Atmospheric Research, 208, 167-179.

Scicchitano, G., Scardino, G., Monaco, C., Piscitelli, A., Milella, M., De Giosa, F., & Mastronuzzi, G. (2021). Comparing impact effects of common storms and Medicanes along the coast of south-eastern Sicily. Marine Geology, 439, 106556.

Scicchitano, G., Scardino, G., Tarascio, S., Monaco, C., Barracane, G., Locuratolo, G., ... & Mastronuzzi, G. (2020). The First Video Witness of Coastal Boulder Displacements Recorded during the Impact of Medicane “Zorbas” on Southeastern Sicily. Water, 12(5), 1497.

Severe Weather Europe (2018). Medicane aftermath in Greece and Turkey: Severe winds, torrential rainfall, major flooding and tornadoes Retrieved from https://www.severe-weather.eu/event-analysis/medicane-aftermath-in-greece-and-turkey-severe-winds-torrential-rainfall-major-flooding-and-tornadoes/

Siahsarani, A., Karami Khaniki, A., Aliakbari Bidokhti, A. A., & Azadi, M. (2021). Numerical modeling of tropical cyclone-induced storm surge in the gulf of oman using a storm surge–wave–tide coupled model. Ocean Science Journal, 56(3), 225-240.

State-of-the-European-climate: November 2019. (n.d.). Retrieved from https://surfobs.climate.copernicus.eu/stateoftheclimate/november2019.php

The National Tidegauge Network of Italy. (2022). Retrieved from https://www.mareografico.it

Tropical cyclones. (2021, April 12). Retrieved from https://public.wmo.int/en/our-mandate/focus-areas/natural-hazards-and-disaster-risk-reduction/tropical-cyclones

UNESCO - Sea Level Station Monitoring Facility. (2022). Retrieved from https://www.ioc-sealevelmonitoring.org

Walsh, K. J., & Ryan, B. F. (2000). Tropical cyclone intensity increases near Australia as a result of climate change. Journal of Climate, 13(16), 3029-3036.

Wettergefahren- Frühwarnung (2019) - information about worldwide extreme weather events. Retrieved from http://www.wettergefahren-fruehwarnung.de/Ereignis/20191114_e.html

# APPENDICES

## A. Meteorological Input Data for Hurricane Dorian

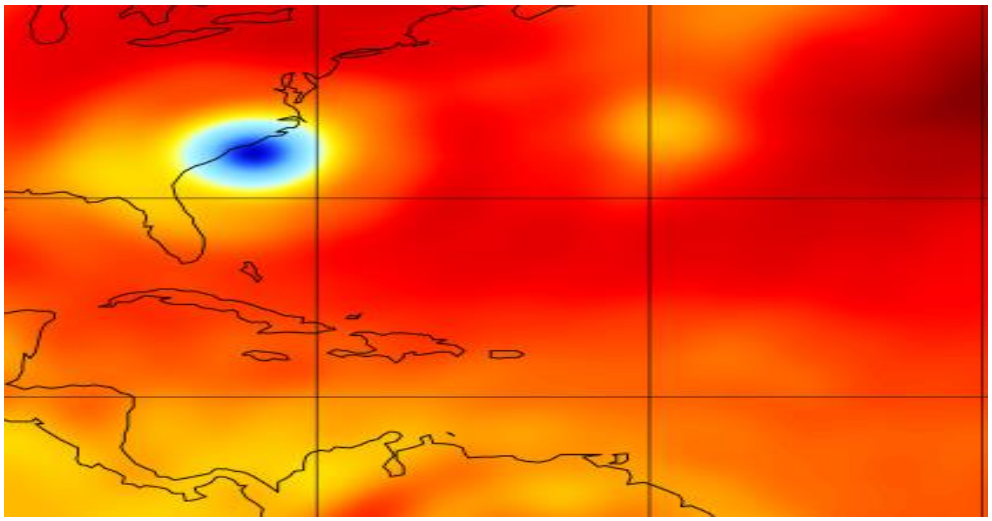

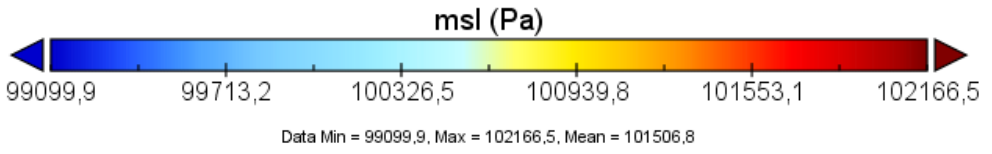


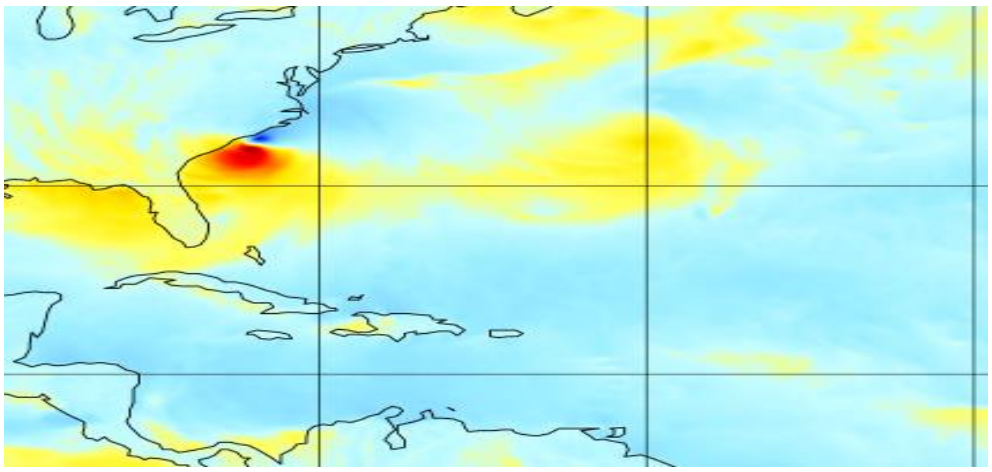

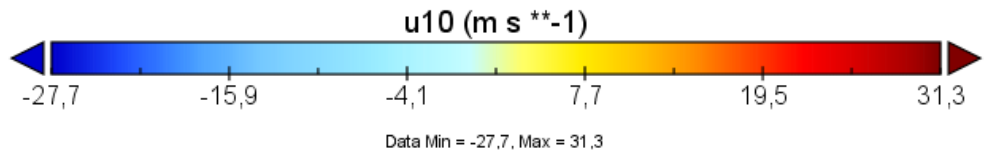

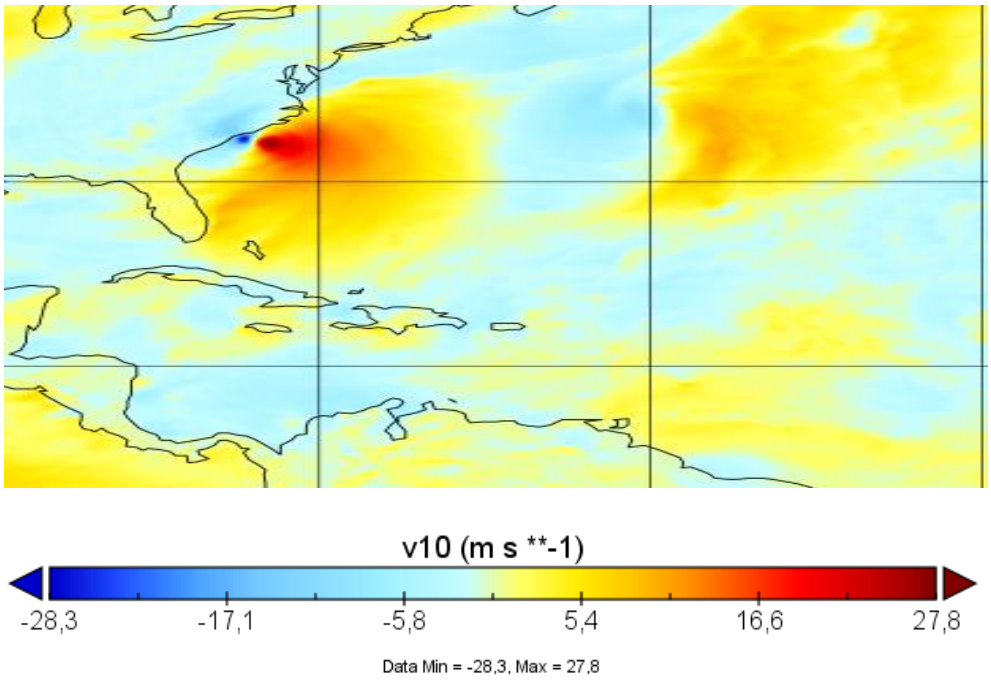


Figure A.1: The atmospheric pressure (msl), eastward wind (u10) and northward wind data (v10) of HRES data set on September 06, 2019 at 00:00 UTC

## B. Meteorological Input Data for Medicane Trudy

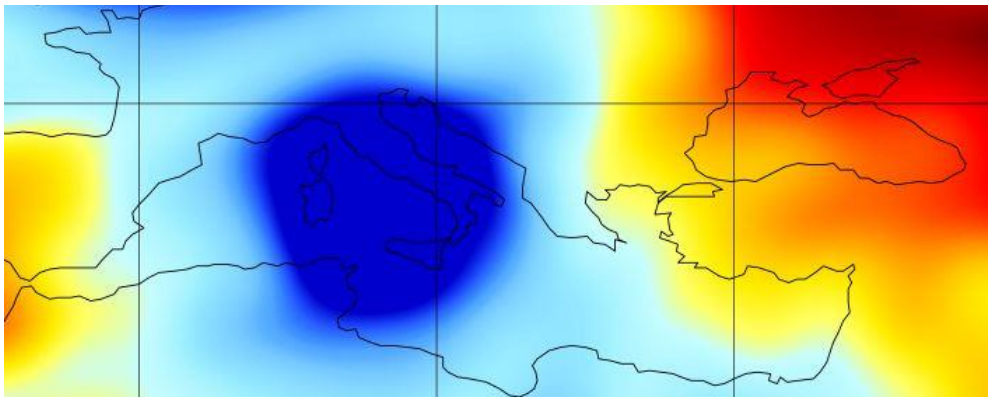

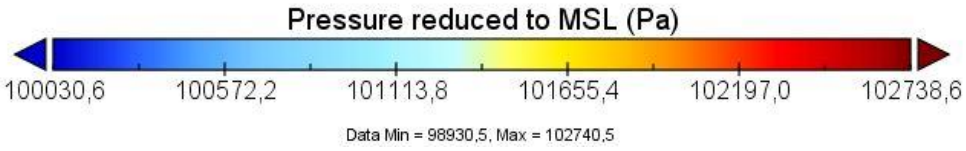


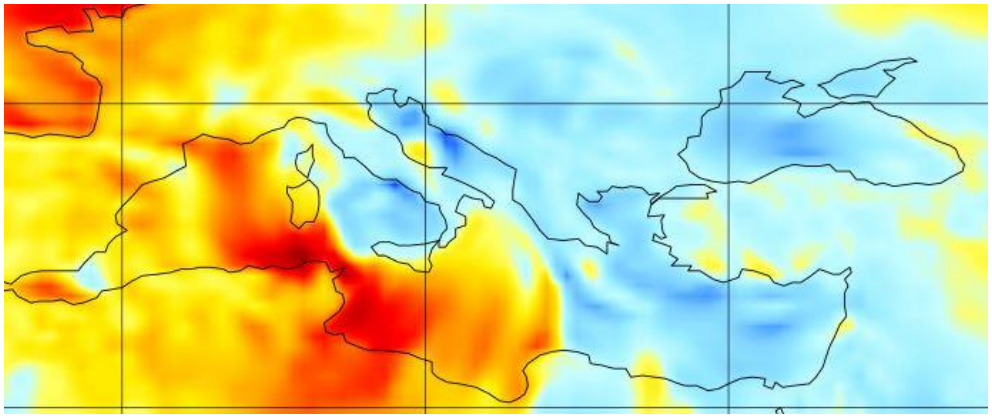

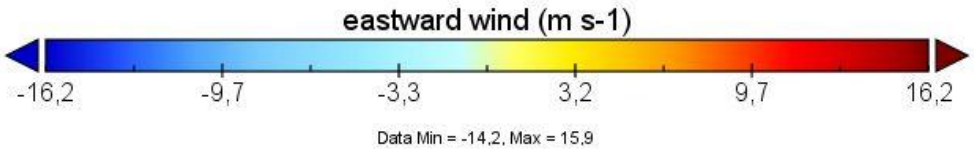

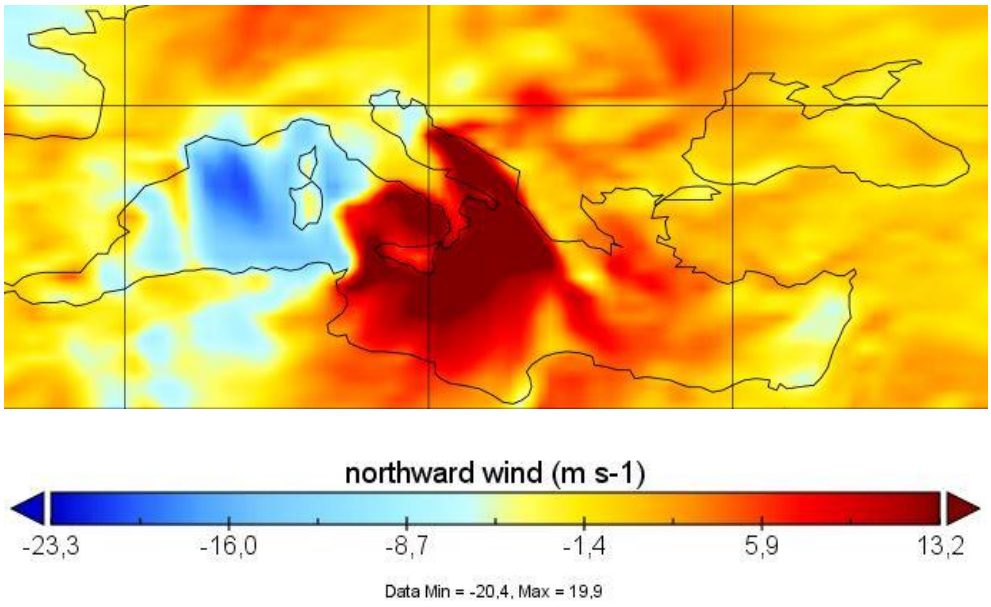


Figure B.1: The atmospheric pressure (msl), eastward wind (u10) and northward wind data (v10) of CFSR data set on November 11, 2019 at 12:00 UTC

## C. Meteorological Input Data for Medicane Zorbas

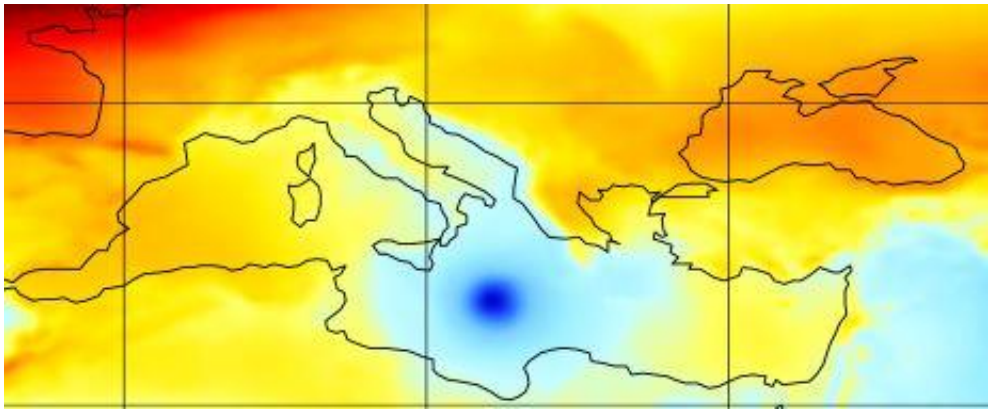

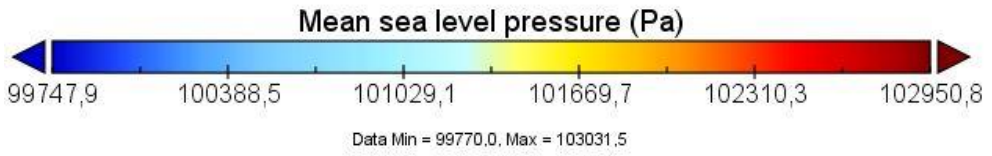


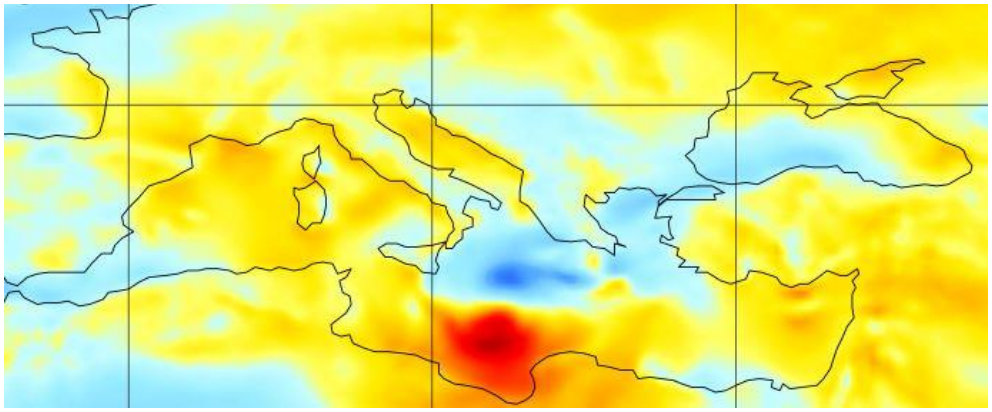

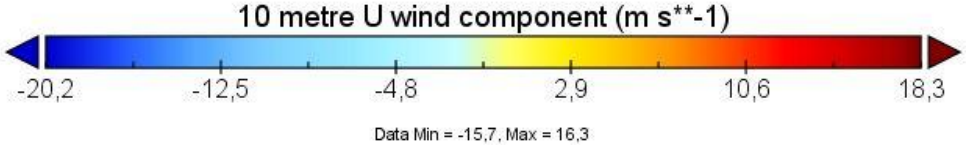

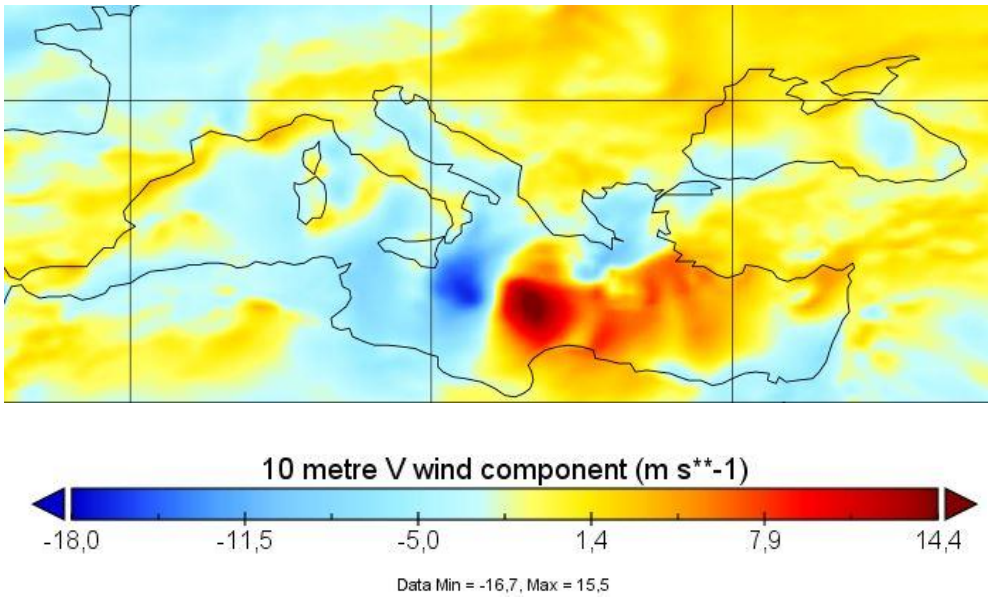


Figure C.1: The atmospheric pressure (msl), eastward wind (u10) and northward wind data (v10) of CFSR data set on September 28, 2018 at 13:00 UTC